

3D printing of hydrogel composite systems: Recent advances in technology for tissue engineering

Tae-Sik Jang^{1#}, Hyun-Do Jung^{2#}, Houwen Matthew Pan¹, Win Tun Han¹, Shengyang Chen¹,
Juha Song^{1*}

¹ School of Chemical and Biomedical Engineering, Nanyang Technological University, Singapore

² Liquid Processing & Casting Technology R&D Group, Korea Institute of Industrial Technology, Incheon, Republic of Korea

Abstract: Three-dimensional (3D) printing of hydrogels is now an attractive area of research due to its capability to fabricate intricate, complex and highly customizable scaffold structures that can support cell adhesion and promote cell infiltration for tissue engineering. However, pure hydrogels alone lack the necessary mechanical stability and are too easily degraded to be used as printing ink. To overcome this problem, significant progress has been made in the 3D printing of hydrogel composites with improved mechanical performance and biofunctionality. Herein, we provide a brief overview of existing hydrogel composite 3D printing techniques including laser based-3D printing, nozzle based-3D printing, and inkjet printer based-3D printing systems. Based on the type of additives, we will discuss four main hydrogel composite systems in this review: polymer- or hydrogel-hydrogel composites, particle-reinforced hydrogel composites, fiber-reinforced hydrogel composites, and anisotropic filler-reinforced hydrogel composites. Additionally, several emerging potential applications of hydrogel composites in the field of tissue engineering and their accompanying challenges are discussed in parallel.

Keywords: hydrogel composites; 3D printing; tissue engineering

*Correspondence to: Juha Song, School of Chemical and Biomedical Engineering, Nanyang Technological University, 70 Nanyang Drive, 637457, Singapore; songjuha@ntu.edu.sg

#The co-authors have equally contributed to the manuscript

Received: September 30, 2017; **Accepted:** November 22, 2017; **Published Online:** January 19, 2018

Citation: Jang T-S, Jung H D, Pan H W, *et al.*, 2018, 3D printing of hydrogel composite systems: Recent advances in technology for tissue engineering. *Int J Bioprint*, 4(1): 126. <http://dx.doi.org/10.18063/IJB.v4i1.126>

1. Introduction

Since the advent of the first three-dimensional (3D) printing system, formerly known as additive manufacturing or rapid prototyping, in 1986, the manufacturing industry has undergone significant transformations, requiring now less time, energy, and producing less waste with the ability to directly fabricate 3D prototypes from computer-aided designs^[1-3]. This fascinating ability to create 3D structures has already taken fabrication technology to a new level, especially in the field of tissue engineering. Over the past two decades, with the development of medical imaging technologies, such as ultrasound, magnetic resonance imaging (MRI), and computed tomography (CT), there

has been multiple attempts to replicate the complexity of anatomical systems in the human body for tissue replacement and regeneration which requires complete restoration of 3D anatomical geometry^[2,4]. However, without artificial or transplant supports, rapid and extensive reconstruction of vital organs in the human body remains a daunting challenge in tissue engineering^[5].

3D printed scaffolds play an essential role in supporting cell adhesion and promoting cell infiltration within their porous matrix^[6]. Moreover, during the tissue reconstruction process, scaffolds are able to provide mechanical support against stressful environments of the human body maintaining sufficient space for the tissue reconstruction and remodeling^[7]. Currently, the most widely used scaffold

materials for 3D printing are hydrogels because they can be easily functionalized or modified, without complex synthesis steps, to replicate the physicochemical properties of most biological tissues^[8,9]. They possess a highly hydrated polymeric structure, exhibiting up to 40-fold change in volume as they swell or shrink in the presence or absence of water, respectively, and can be modified to respond to various physical and biological stimuli such as temperature, light, pH, ions, and biochemical signals^[9,10]. These unique features make hydrogels excellent environments for cell attachment and proliferation within their hydrated hydrogel networks, which offer abundant space for cell growth while facilitating the transportation of essential metabolites and nutrients to the encapsulated cells^[8,11]. However, most hydrogels suffer from a lack of mechanical strength and unsuitable degradation behavior compared with native tissues such as ligament, tendon, muscle, or cartilage. Therefore, augmenting the mechanical properties and bioactivity of hydrogel have been a challenging task for material scientists^[8].

Hydrogel composite system is one of the most suitable strategy for incorporating and combining various hydrogel functions and properties, not attainable by any single hydrogel alone^[11]. Over the past few decades, a diverse range of reinforcements have been proposed utilizing various composite designs such as particle-, anisotropic filler-, and fiber-hydrogel composite systems in which reinforcements are stabilized and immobilized via physical or chemical interactions in the hydrogel matrix^[8,9,11,12]. In the case of hydrogel-hydrogel composite system, the interpenetration between the two polymer networks forms a mechanical anchoring behavior, and these complexes strongly affect the hydrogel rheology, degradation rate, permeability, and mechanical properties^[13]. Conventional inorganic reinforcements are based on physical interactions with the hydrogel matrix in which secondary or van der Waals forces including London dispersion forces, dipolar interactions and hydrogen bonding are involved^[14]. These physical interactions generate strong adhesion between the reinforcements and hydrogel matrix, and the enhancement of hydrogel properties are dependent on the amount of reinforcements and the volume ratio of physically interacted- and non-interacted-polymer networks^[15]. In the case of chemical modifications, the introduction of chemical groups and the covalent bonding formations at the interface induce superior interfacial bonding strength of which energy is generally in between the 40 to 400 kJ/mol *i.e.* much higher than physical interaction (8–16 kJ/mol)^[14]. Thus, it is possible to provide substantial increase of mechanical strength to the hydrogel composite system.

While the hydrogel composite has attracted a lot of attention due to its superior properties, most review articles report on conventional fabrication techniques such as molding or casting^[5,7]. Compared with well-

understood and evaluated conventional manufacturing processes, hydrogel composite 3D printing systems remain a relatively new area of research and much more can be studied with regards to their physicochemical properties such as viscosity, dispersion, reinforcement, and its size and shape^[16,17]. In recent years, significant progress has been made in the development of 3D printing systems for hydrogel composites with improved mechanical performance and biofunctionality^[1,16,17].

Herein, we first provide a brief introduction of hydrogel composite 3D printing techniques and their application in the field of tissue engineering. We shall categorize 3D printing into (a) laser based-3D printing, (b) nozzle based-3D printing, and (c) inkjet printer based-3D printing systems, and discuss their working principles and recent trends. In particular, we will discuss four different hydrogel composite systems: i) polymer- or hydrogel-hydrogel composite, ii) particle-reinforced hydrogel composite iii) fiber-reinforced hydrogel composite, and iv) anisotropic filler-reinforced hydrogel composite, and highlight tailored physical properties and their functionality. Additionally, several emerging potential applications of hydrogel composites in the field of tissue engineering and their accompanying challenges are discussed in parallel.

2. 3D Printing Technology for Hydrogels Composite

2.1 Laser-based Hydrogel 3D Printing Systems

Most laser-based 3D printing systems are applicable for the hydrogel composite fabrications, which builds a 3D structures in a vat of photocurable hydrogels under the deposition of laser energy, usually UV range, in specific designed patterns^[3]. The exposure of UV laser on to the surface of photocurable liquid causes gel-formation of a thin single layer, and it is sequentially moved upward or downward with the sample stage to allow the next layer formation on top of preformed structure. During this process, designed 3D structures are directly materialized in the liquid vat that means the hydrogel composites can be built within the photocurable organic-inorganic solution^[3,18,19].

Since the development of laser-based 3D printing in 1980s, several other commercially available techniques have emerged, and they are widely used for biomedical applications such as scaffolds, drug delivery, implants, and devices^[2,18]. Laser-based 3D printing system can be divided into several categories based on the type of laser source, beam delivering system, method of scanning or exposure, and type of stage movement system. However, most of these techniques require post-processing such as support removal and other unwanted materials. In addition, a post-curing procedure is necessary to completely cure the built structure for intact mechanical

stability. In this chapter, basic principle of popular laser-based 3D printing techniques for the hydrogels will be further discussed.

2.1.1 Stereolithography Apparatus

Stereolithography apparatus (SLA) is one of the most widely used 3D printing systems based on the layer-by-layer solidification of a liquid photocurable hydrogel. Computer-controlled UV-laser is scanned across the surface of the liquid hydrogel in a vat, and that leads to the formation of the covalent bonds between the adjacent chains of photocurable polymers resulting in a solidified single layer of the designed 2D pattern. The platform then descends a distance equal to the thickness of a single layer of the design to fully re-coat the surface of the preformed 2D pattern with fresh liquid hydrogel^[3]. This procedure is repeated until the 3D object is complete, as shown in (Figure 1A). Interconnection between the 2D

patterns of each layer can be achieved in the precisely controlled optical scanning system with slightly larger focusing depth than the one-layer height^[3,18].

Generally, SLA 3D printing system has many advantages such as wide range of building volume (from 200 to 2000 mm), high structural resolution, and good quality surface finishes. In addition, high accuracy and consistency of 3D printed objects could be achievable by controlling UV-laser power, scanning speed, exposure time, spot size, and wavelength^[2,18]. Despite its advantages, the limited range of photocurable hydrogels, requirement of support structures, and post-curing process are the major drawbacks of SLA techniques in hydrogel composite fabrication.

More recently, the resolution of SLA has been improved by a complex optical system for the beam delivery. With this micro fabrication technique of SLA, also known as micro-stereolithography (μ SLA), light beam can be focused into a spot size of few micrometers, which requires

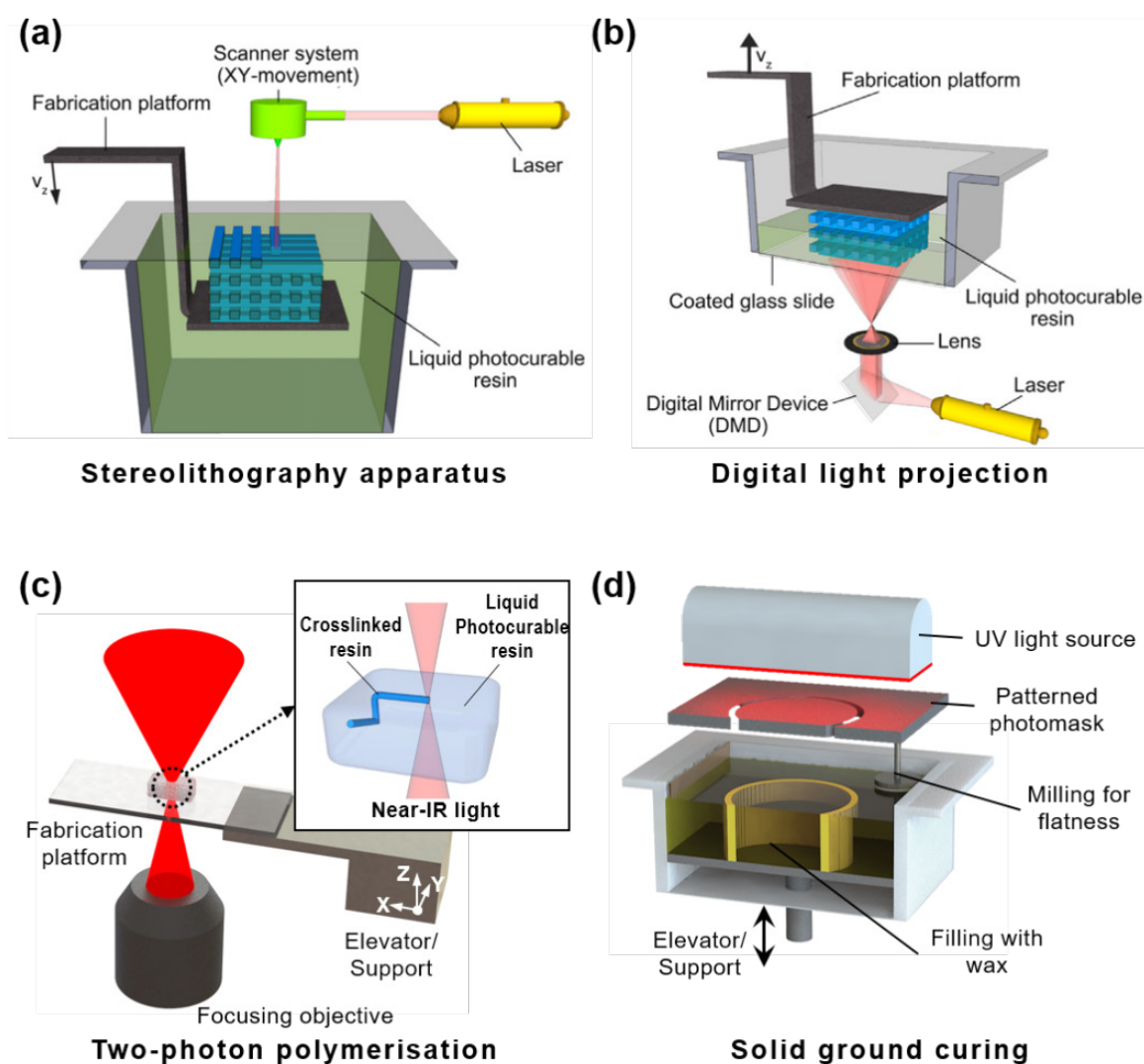


Figure 1. Schematic images of laser based hydrogel 3D printing systems.(reproduced with permission from [3]. Copyright 2012, Elsevier Ltd).

precise beam controlling and scanning system^[19]. So far, μ SLA can be categorized into (i) scanning μ SLA system and (ii) mask (or integral) projection μ SLA system. In the scanning μ SLA, UV beam is fixed with a stationary spot position onto the liquid hydrogel surface, and scanning is conducted by moving the work piece stage including the vat, which can eliminate the unstable mobile optical elements leading to focusing errors and poor resolution^[20,21]. In the mask projection system, light beam exposure of each liquid hydrogel layers is conducted in a single radiation using dynamic pattern generator mask. The sliced 2D patterns of 3D structure is converted into a data file and input to the light beam mask, which can generate the precise patterns corresponding to the each layer of structure^[22,23]. The patterned beam is focused by the computer-controlled focusing optical components to reduce the whole pattern size into micrometers. The highly precise 3D structure containing complex engineered shapes can make a unique interface between the nano-scale functional second materials and macro-scale hydrogel molecules, which provides an engineering platform for various industries, such as tissue engineering, photonics, and microelectromechanical system (MEMS)^[19,23].

2.1.2 Digital Light Projection

Digital light projection (DLP) is developed from the mask projection system of SLA. However, in this 3D printing system, digital mirror device or liquid crystal displays play a role of dynamic pattern generator mask, which consists of several millions of arrayed mirror or LCD pixel units to generate an individual on-off beam signal (Figure 1B). The DLP light source allows fabrication of the 3D structure with high resolution between 25 and 150 μ m, which can be further enhanced with additional multi lens components to focus the light beam sources^[2,3,18]. In comparison to other 3D printing systems that have bottom-up construction approach, DLP is based on a top-down working principle^[24]. The beam source is placed at the bottom part of system, photocurable liquid hydrogel is exposed by the beam through the transparent contact window underneath the vat. The building plate or carrier is immersed into the liquid hydrogel and moves vertically upward direction after each layer is polymerized. In this process, fresh liquid hydrogel is automatically supplied to the bottom layer through the capillary action, and each repetitive processing steps can be conducted within 15 seconds^[2,3]. In the DLP system, any planarization or levelling process is not required which allows to increase the building speeds and thus eliminate the fabricated parts from damaging during the wiping actions.

2.1.3 Two-Photon Polymerisation

Two-photon polymerisation (TPP) is an entirely new

stereolithographic strategy to fabricate nanoresolution structures without undergoing the layer-by-layer process. The light source of TPP system is femtosecond infrared laser pulses that is focused into the volume of photocurable liquid materials, and initiates photolytic polymerization process without any masks^[3,18,25]. In contrast to the UV light, nonlinear behavior and existence of polymerization threshold intensity of infrared light allow direct fabrication of complex 3D structure inside the photosensitive liquid with much higher structural resolution as high as 200 nm. Thus, 3D printed objects by TPP obtain better quality than the parts fabricated by conventional stereolithography techniques, as shown in (Figure 1C)^[3,18]. Because of its ultra-small focusing spot size, the scanning of tightly focused beam of ultra-short laser pulse is precisely controlled by a computer positioning system combined with piezoelectric stages and/or optical scanning systems. The high intensity of photons from the two-focused beam source causes excitation of the photoinitiator molecules resulting in the creation of free radicals. These free radicals break the unstable bond of monomers and initiate the polymerization process. As a result, polymer chains can be formed and grown by combining monomers and adding to the chains. Although conventional photosensitive materials and initiators have been developed, such polymer still suffers from the insufficient free radical density within the extremely small cross-sectional focusing area for two-photons^[26,27]. Thus, enough duration of each scan position, high density of photoinitiator, and intensity of focused light beam are most important parameters to terminate the photopolymerization procedure with enough crosslinking density.

TPP is promising 3D printing technique for biological applications, such as drug delivery, implants, biosensors, and tissue engineering. Since infrared light does not cause any harmful effect to the living cells or organisms, customized 3D scaffold structure can be directly fabricated in the presence of living cells^[28]. Furthermore, it allows the introduction of pores at any location within the structure, which enables precise control of the cell position, movement, interaction, and organization inside the scaffold and, consequently, integrity with host tissue inside the body^[18,27,28]. For the practical application in tissue engineering, hybrid materials with either organic/organic or organic/inorganics are consistently introduced for the better cell affinity and biocompatibility of 3D printed scaffolds.

2.1.4 Solid Ground Curing

Solid ground curing (SGC) is one kind of projection beam systems developed by Cubital Inc. in 1986. In this system, the fabrication of the each layer patterns of 3D object is done by a high-powered UV lamp in the presence of the patterned mask over the surface of photocurable materials^[18,29,30]. The patterned mask is

built by the machine prints on the glass plate, and placed in between the light source and the fabrication platform. The fabrication principle of this technique resembles the previous SL printers, but it has unique features of process and support material design. Every fresh photocurable materials are coated on top of fabricated structure by spraying method. After UV light irradiation on the liquid materials, uncured material is removed by vacuum and filled with a wax as a supporter for the next layer (Figure 1D). During these repeating this process, planarization or levelling procedure of coated new layer is necessary for the accurate and reliable finishing. After printing, the wax is melted away from the 3D structure^[18,29].

2.2 Nozzle-based Hydrogel 3D Printing Systems

Nozzle-based printing method is the most popular technique to build hydrogel based scaffolds. The melted polymers or viscous liquids are forced and extruded out of a nozzle, syringe or orifice and solidified onto a building stage as shown in (Figure 2A). 3D structures are constructed through sequential extruding material layer-by-layer which follows a pre-designed path constructed by computer modelling. The key to successful 3D printed structures using this method is good interlayer adhesion between layers. Hence, various parameters of hydrogels such as solidification temperature, rheological properties and the gel setting mechanism are critically important. In extrusion-based printing, polymers must be either viscous or viscoelastic initially. These printed layers are cured and become self-supporting hydrogels before next layers are printed.

Nozzle-based printing can be categorized into two groups: techniques with melting process and techniques without melting process. Nozzle-based printing with melting process include fused deposition modelling (FDM), precise extrusion manufacturing (PEM), multiphase jet solidification (MJS), precision extrusion deposition (PED), and 3D fiber deposition^[31–34]. FDM technique is the most commonly used nozzle based 3D

printing method in which thermoplastic filaments such as poly(lactice acid) (PLA) and acrylonitrile-butadiene-styrene (ABS) are melted by heating and extruded on the build plate^[35]. However, all techniques with a melting process are not suitable processes to deposit hydrogel since applying heat to hydrogel can cause a decrease in biocompatibility and thermal degradation^[3,36]. Heat treatment for sol-gel transition of hydrogels at elevated temperatures induces critical damage to cells loaded in the hydrogels, resulting in acute cell death^[37]. In addition, unlike thermoplastic polymers, hydrogels are in the form of viscous liquid and cannot be used as materials for FDM as they cannot be shaped into filament due to their poor mechanical properties.

Therefore, most of hydrogel-based 3D printings studies are performed by printing techniques without melting process including five major categories, 3D biplotting, pressure-assisted microsyringe (PAM), direct ink writing (DIW), low-temperature deposition modelling (LDM), and robocasting, based on the proposed categorization of nozzle-based printing systems by Billiet *et al.*^[3] These printing techniques allow rapid fabrication of structure with improved mechanical integrity. Moreover, they have been widely used for extrusion of hydrogel-based composites as well as hydrogels with drug or cell delivering capabilities. These techniques without melting process can be further classified by their working principles such as mode of extrusion, nozzle design, and type of materials as described in the following section.

2.2.1 3D Plotting

In 2000, Freiburg Materials Research group first developed 3D plotting method to produce scaffolds for soft tissue engineering^[38]. 3D plotting method uses viscous hydrogels which are initially loaded in a syringe and injected through a micro-needle used as the extrusion nozzle into a liquid solution with a density similar to that of the hydrogel. The hydrogel from a pressurized syringe can be deposited as a single continuous microstrand or as individual

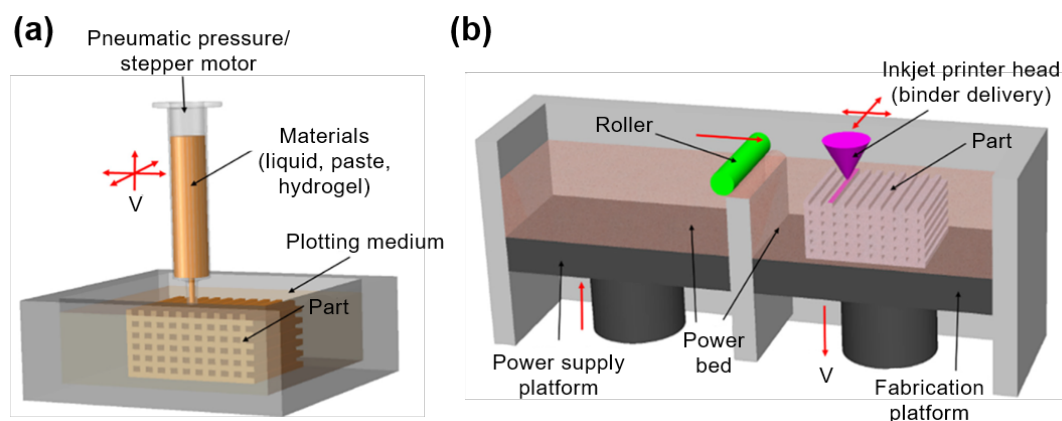


Figure 2. Schematic images of (A) nozzle and (B) inkjet printer based hydrogel 3D printing systems. (reproduced with permission from [1]. Copyright 2017, Elsevier Ltd)

microdots. The thickness of microstrand can be controlled by the viscosity of hydrogel, deposition rate, diameter of nozzle, and applied pressure. The material dispensing head generally moves in x, y, z directions, while the build platform is kept in place. Liquid flow is generated by working stepper motor (volume-driven injection nozzle) or filtered air pressure (pneumatic nozzle). The key point of this technique is to plot hydrogel into a liquid solution with a carefully designed density that matches that of the hydrogel.

Various materials can be used in 3D plotting system such as hydrogels, nanocomposite hydrogels, polymer sol, and bioactive polymers such as proteins^[39-42]. Materials with low viscosity can also be used in plotting since deposition takes place in a liquid medium with a matching density. Moreover, thermal sensitive biocomponents such as growth factor and even cells can be incorporated into hydrogels because heating is not required. Extruded hydrogels can be cured by plotting in a reactive solution or by using mixing nozzles with multiple dispensing component. However, the microstrands of scaffolds constructed by 3D plotting technique normally possess smooth surfaces, which cause unfavorable environment for initial cell adhesion. Thus additional surface treatment has been researched for fabricating the favorable surface with modified initial cell adhesion^[43].

2.2.2 Direct Ink Writing (DIW)

Direct ink writing (DIW) or direct write assembly (DWA) was first investigated by Lewis *et al.*^[44] A variety of inks such as hydrogels, nanoparticle filled inks, colloidal suspensions and gels, and organic inks can be printed in 2D and 3D patterns with feature sizes ranging from 100 nm to 1000 μm . Components of DIW apparatus are the three-axis translation platform, compressed air supply, cylindrical nozzle, and optical microscope for real-time monitoring. The hydrogels are stored in each orifice mounted on the Z direction motion stage and printed through a nozzle onto a moving XY stage. The pressure of orifice and printing speed depend on nozzle diameter and rheology of hydrogel, respectively.

There are two important considerations regarding the hydrogels used in DIW technique. First, they must obtain self-supporting ability and spanning shapes with controlled viscoelastic characteristics. Therefore, extruded hydrogels should set instantly to enable feature retention of the printed structures. Second, high concentration of nanoparticle or colloid in hydrogels is preferred to reduce shrinkage during the drying process of the completed assembly. Generally, 70–85 wt% of solid loadings in hydrogels are preferred for assembling planar and spanning filaments^[45]. The nanoparticle or colloid network in hydrogels is able to resist compression stress caused by capillary tension, thereby preventing

spreading during extrusion.

2.2.3 Pressure-assisted Microsyringe (PAM)

The PAM technique, similar to FDM without heating system is first proposed by Vozzi in 2002^[46]. In the initial stage, pneumatic driven glass capillary microsyringe which moves in the vertical plane was used to deposit materials on a substrate. Vozzi and his research group modified PAM systems for hydrogel microfabrication^[47]. Compressed air and pneumatic driven microsyringe were replaced with a stepper motor and piston assisted microsyringe, respectively. Moreover, a temperature controlled syringe module with an aluminum jacket was added to control the temperature of deposit materials.

2.2.4 Low-temperature Deposition and Manufacturing (LDM)

Xiong *et al.* designed LDM systems to overcome heating process^[48]. In this technique, temperature is decreased to solidify materials. Materials such as hydrogels are embedded in feeder connected to a screw pump nozzle and injected from the nozzle that can move along the XY axis onto a building stage at a temperature below 0 °C. Printed scaffolds are necessary to undergo freeze-drying process to remove the solvent. Modified LDM technique, called multinozzle low-temperature deposition and manufacturing (M-LDM) was developed by incorporating multiple nozzles with different types^[49]. They are used for fabrication of scaffolds with gradient structures and materials by the incorporation of additional jetting nozzles into the LDM process.

2.2.5 Robocasting

Robocasting is also a nozzle based process which was originally adapted to produce ceramic scaffold using highly loaded ceramic slurries^[50]. The system is composed of stationary dispensing head and movable platform that can move in X, Y and Z axis. The slurry injected layer by layer from a syringe has to sustain their weight and the weight of next layers to sustain the printed features. Thus, low viscous slurry or hydrogel alone are inadequate for robocasting technique. Recently, hydrogels were applied as carriers for ceramic powder in this system. Although the final product is a ceramic scaffold that is formed through burning out hydrogels, this result indicates the great potential of robocasting process in fabrication of hydrogel-based composites.

2.2.6 Other Apparatus

Nozzle-based 3D printing process is a promising technique to fabricate hydrogel-based composite scaffolds due to its versatility in various printing conditions. This technique is capable of printing large porous structures for infiltrating body fluid and controlling mechanical and biological properties, which cannot be carried out by other hydrogel

3D printing techniques. However, there are some drawbacks such as limitation of material type, nozzle condition, and natural ability of this process hinder its potential.

To date, scaffolds fabricated by nozzle based 3D printing technique show low resolution and poor mechanical properties. Compared to laser based 3D printing and droplet based 3D printing technologies, the resolution of nozzle based 3D printing is relatively low. Moreover, the resolution is dependent on the solid loading or particle size on hydrogel-based composites. As the hydrogel is extruded from the nozzle, it does not have the material strength to maintain the structure and result in sagging or collapse of unsupported parts. This phenomenon of mechanical property deterioration is aggravated during the printing process of scaffolds without the assistance of supporting materials or liquid medium. When the hydrogel materials possess sensitive biocomponents such as cells or ECM or growth factor, low printing speed and external pressure on materials may lead to function loss or damage of biocomponents.

For solving these disadvantages, other improved and combined nozzle based systems have also been reported steadily. Multi-head deposition system (MHDS), bioExtruder, screw extrusion system (SES), combined rapid freezing and plotting system, modified plotting system and porogen-based extrusion system are some of the novel attempts^[51-56]. These techniques were investigated to enhance manufacturing flexibility by increasing the capability of deposition in accomplishing optimum scaffold requirements.

2.3 Inkjet Printer-based Hydrogel 3D Printing Systems

3D printing technology, also known as additive manufacturing, originated from 2D inkjet-based printer. It was first developed at the Massachusetts Institute of Technology (MIT) in 1993 by depositing liquid binder onto a powder bed^[57]. Inkjet printer is a non-contact technology which prints droplets of ink onto a material platform. It is composed of a printer head which possesses liquid binder cartridge and moves in the XY plane and a build platform that is movable along the Z axis as shown in (Figure 2B).

Inkjet printing process can be divided into two types; continuous inkjet (CIJ) printing and drop-on-demand (DOD) printing^[58,59]. In CIJ printing, liquid binder emerges continuously from a nozzle to form a jet which breaks up into droplets by the Rayleigh instability, whereas individual droplets are ejected only when electrical signals result from thermal or piezoelectric effect in DOD printing. Both systems offer droplets ranging in size from 15 to several hundred microns. However, DOD printing is preferable for fabricating biological structures of soft tissue engineering applications due to the reduced possibility of contamination

and good controllability^[60].

As mentioned above, piezoelectric or thermal force is used to eject liquid drops in DOD printing systems. In piezoelectric inkjet printer, the application of external voltage to piezoelectric actuator generate pressure to eject droplets from nozzle. Thermal inkjet printer, which possesses low cost, high print speed, and wide availability, uses an electrical heating to generate pulses of pressure that leads to the vaporization of liquid. Application of air-pressure pulses eject small droplets from the nozzle. Heating temperature is usually in the range from 200 °C to 300 °C, which can lead to denaturalization of hydrogels or biocomponents in hydrogels. However, due to the short heating time (~2 μs) in the printing process, heating has shown no detrimental effect on the stability of biocomponents in recent studies^[61].

Similar to other 3D printing techniques, hydrogel scaffolds pre-designed by computer modeling are constructed layer-by-layer with deposition materials. And there are a variety of material that can be used in inkjet 3D printer. These can be categorized in two types by starting materials on platform as described in the following section.

2.3.1 Inkjet Based 3D Printer with Powder (I3DP-P)

I3DP-P system (Figure 3A) is the representative solid-phase rapid prototyping technology. This system can use various materials including ceramic, metals, polymers as well as hydrogels^[62-65]. The process is a 3-step process. The first step in 3D printing is the spreading of powder onto a platform with a roller. Second step is the deposition liquid binder from inkjet print head with a 2D pattern onto the powder layer by bonding the adjacent powder particles together. The final step involves lowering the layer and filling the powder on the next layer. This process is repeated until the fabrication process is completed. The unreacted powder with binders can support the bonded structures, thus no supporting material is needed. Various types of powder such as a single powder, surface-coated powder, and a mixture of different powders are used in this system. Selection of suitable biocompatible powder and binder is the most important part in I3DP-P system.

2.3.2 Inkjet-based 3D Printer with Liquid (I3DP-L)

There are two types of I3DP-L (Figure 3B). The working principle of the first type is similar to the I3DP-P system but the powder bed is replaced by liquid materials^[66], and the second type is a direct inkjet writing system which generally uses photosensitive resins^[67]. In the case of the former system, uncrosslinked hydrogels are filled in bed platform which moves along Z-axis and the liquid crosslinker ink such as calcium chloride are printed from the print head. In direct inkjet writing systems, photosensitive resin ejected from inkjet printer head build are constructed by simultaneous curing with light. Compared with I3DP-P, fabricated scaffolds shows high

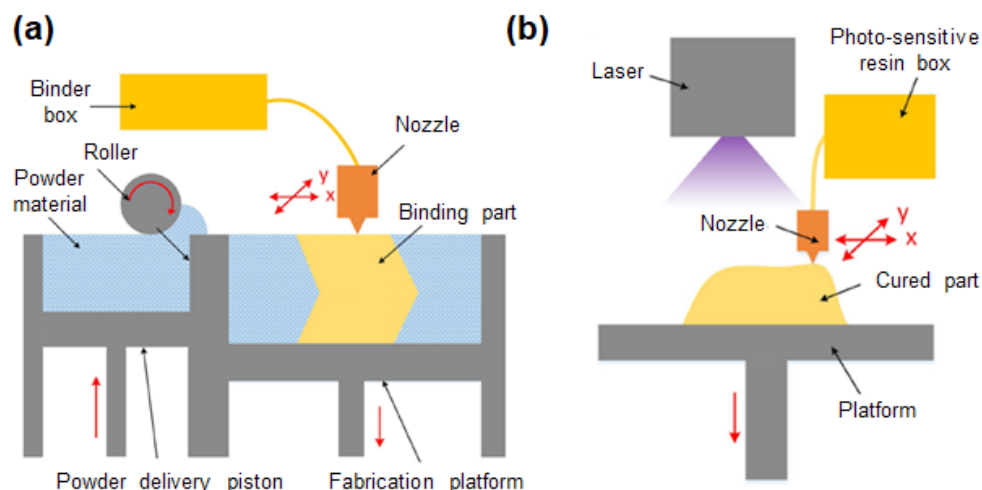


Figure 3. The schematic images of (A) I3DP-P and (B) I3DP-L printer based inkjet 3D printing system. (adapted with permission from [139]. Copyright 2016, John Wiley & Sons, Ltd).

accuracy, but the cost of I3DP-L is higher.

A wide range of materials can be used with both Inkjet-based 3D Printer with powder and liquid as these processes are done in room temperature. Moreover, these techniques offer more options for soft tissue engineering and bioprinting because incorporated biocomponents are not subjected to deleterious effects of laser-mediated fusion or force by extrusion. However, post processing is required as water soluble liquid binders often remain after 3D printing. In addition, it is difficult to remove internal unbound powder or liquid which were trapped in the negative spaces such as hollow structures.

3. 3D Printing of Hydrogel Composites

Hydrogels provide many advantages for tissue engineering and cell delivery applications owing to their tunable degradability, biocompatibility, and capacity to be modified. However, their inherently poor mechanical properties make them unsuitable for applications requiring strength such as load bearing components. The rapid biodegradation behavior of hydrogels also has greatly limited their further application in the tissue engineering. In addition, in the case of biodegradable synthetic hydrogels with polyester chains, acidic by-products during the hydrolysis degradation process of ester bonds were found to induce the side effects to the cells^[68]. Therefore, the addition of materials including metals, ceramics and polymers were essential to improve some of the limitation of hydrogels.

Printability is one of the most important criteria to consider for 3D-printing of hydrogel based composites. It plays a critical role in determining the degree of accuracy and precision relative to the computed spatial and temporal design. The printability of hydrogel composites requires

stimuli-dependent viscosity to be used in various printing methods which may involve changes in temperature and shear thinning to prevent the nozzle from clogging and to maintain the intended shape after printing. Research has reported the addition of ceramic or metal based nano or microparticles as rheology modifiers often interrupt the crosslinking of hydrogels, thus decreasing the printability of materials^[69]. In addition, the incorporation of these additives may lead to a decrease in the accuracy of printed scaffolds due to an increase in nozzle size or even make the resulting material completely unusable. Therefore, many studies have tried to print hydrogel scaffolds by incorporating additional hydrogels, soft polymers or inorganic second phases.

3D printing techniques for the fabrication of hydrogel composites can be categorized into (i) polymer or other hydrogel reinforced composite (ii) particle-reinforced composite (iii) anisotropic filler-reinforced composite, and (iv) fiber-reinforced composite hydrogel printing systems, as represented in Table 1. It should be noted that for the category (i), hydrogel-reinforced composites, matrix and reinforcement materials were defined based on the volume fraction of hydrogels in the composites according to our framework. For instance, if gelatin has a higher volume fraction than alginate does in their composite, we assume that gelatin is the matrix and alginate is the reinforcement for this gelatin-alginate composite. These categories will provide a platform for designing an appropriate combination of materials and 3D printing technique for achieving the desired properties. Each system involves an innovative combination of reinforcement and hydrogel matrix that generate not only mechanical strengthening but also a plurality of property enhancements such as biological activity, degradation tunability, and enzyme sensitivity.

Table 1. The summary of methods and materials for 3D printing of various hydrogel composites

Reinforcement type	3D printing methods	Matrix materials	Reinforcement materials	Properties	Potential application	Ref.
Gel	3D plotting	Alginate	Poly(acrylamide)	Improved tensile properties	Tendon	[70]
	3D plotting	Gelatin	Alginate	Maintained tensile biomechanics	Aortic heart valve	[17]
	3D plotting	Collagen	Gelatin	Formed vascular construct with cell	Vascular tissue	[71]
	3D plotting	PEGDA	Alginate	Improved toughness	General	[72]
	3D plotting	Alginate	Nanocellulose	Improved storage modulus	Cartilage (Ear)	[73]
	3D plotting	PEGX	Gelatin	Improved storage modulus and critical strain	General	[74]
	3D plotting	Gelatin-alginate	Fibrinogen	Improved cell differentiation and self-organization	Drug discovery	[75]
	3D plotting	Alginate	Gellan gum	Improved swelling ratio and stiffness	General	[76]
	3D plotting	PCL	PEG, HAc	Improved storage modulus	General	[77]
	3D plotting	PEG	P(HPMAm-lactate)	Improved rheological properties and degradation rate	Cartilage	[78]
	DIW	HAc	Glycidyl methacrylate	Improved mechanical properties	General	[79]
	LDM	Collagen	PU	Improved nerve regeneration capability	Nerve conduit	[80]
	Robocasting	Chitosan	Alginate	Large-scale structures	General	[81]
	Inkjet printer	Alginate	Gelatin	Cell printing	General	[66]
	Inkjet printer	Starch	Cellulose, Dextrose	Improved elongation	General	[65]
	DLP	PU	HAc	Improved degradation rate	Cartilage	[82]

Table 1. (continued).

Reinforcement type	3D printing methods	Matrix materials	Reinforcement materials	Properties	Potential application	Ref.
Particle	3D plotting	Alginate, Gelatin	Bioglass (55 nm)	Improved cell proliferation and mineralization	Bone	[83]
	3D plotting	Methacrylated chitosan	Graphene oxide (430–460 nm)	Improved elastic modulus, tensile strength and conductivity	Biomedical device	[84]
	3D plotting	Alginate, Gelatin	Hydroxyapatite (183 nm)	Improved mechanical properties and biological properties	Bone	[85]
	3D plotting	Thiol-modified hyaluronic acid	Gold nanoparticle (24 nm)	Decreased gelation time, and improved mechanical properties	Vessel	[86]
	3D plotting	Alginate	Biphasic calcium phosphate (106–212 μm)	Improved biological properties	Bone	[87]
	Inkjet printer	Natural polysaccharides gums	Carbone nanotube (10 nm)	Improved radiopacity and conductivity	Biomedical device	[88]
	Casting + FDM	GelMA	PLA 3D structure (200 μm)	Improved mechanical properties	Bone	[89]
	SLA	PEGDA	Hydroxyapatite (50–100 nm)	Improved biological properties	Bone	[90]
	SLA	PEGDA	Hydroxyapatite (80–100 nm)	Improved mechanical properties and biological properties	Cartilage	[91]
	Fiber	3D plotting	Acrylamide	Cellulose short fibril	Anisotropic swelling behaviors	4D printing
3D plotting		Alginate	PLA continuous nanofiber	Improved mechanical properties and biological properties	Cartilage	[93]
Casting + 3D plotting		PEGDGE, Acrylamide	PU continuous microfiber	Improved mechanical properties	General	[94]
3D plotting		Alginate, Acrylamide	Emax (UV-curable epoxy)	Improved mechanical properties	Cartilage	[95]
Anisotropic filler	DIW	PEGDA, alginate, gelatin	Laponite RD, Laponite XLG	Improved self-supporting capacity and young's modulus	General	[96]
	3D plotting	N-acryloyl glycinamide	Laponite XLG	Improved tensile and compression properties and biological properties	Bone	[97]
	3D plotting	Alginate-methylcellulose	Laponite	Improved shape fidelity and sustained drug delivery	Bone	[98]

3.1 Polymer or Other Hydrogel Reinforced Hydrogel Composites 3D Printing

Hydrogels for 3D printing can be divided into protein-based natural hydrogels such as gelatin, collagen, silk or polysaccharide-based natural hydrogels such as chitosan, agarose, hyaluronic acid (HAc), alginate, cellulose, or synthetic hydrogels such as poly(ethylene glycol) (PEG), polyurethane, polyacrylamide. Alginate, a common hydrogel crosslinked by ionic interactions or phase transition, has been widely used in the field of

soft tissue engineering owing to their biodegradability and low toxicity. However, alginate limits cellular adhesion due to the lack of adhesion sites for cells. Markstedt *et al.* investigated 3D printing materials for cartilage tissue engineering applications by combining alginate and nanofibrillated cellulose^[73]. Their rapid cross-linking ability and the shear thinning properties make the scaffolds fabricated by 3D plotting method stable. Human nasoseptal chondrocytes encapsulated in nanofibrillated cellulose/alginate hydrogels exhibited

86% of viability at day 7 after 3D culturing. Xu *et al.* fabricated a composite extracellular matrix by printing alginate/gelatin hydrogels with incorporating fibrin which is a natural scaffold material^[75]. Fibrin acted as an important component to regulate self-organization and differentiation of adipose derived stromal cell. This printed hydrogel composite functions as an extracellular matrix that can offer an environment for cell growth and a platform for drug delivery in soft tissue engineering. The gellan gum, a versatile gelling agent, was introduced as compounding materials in 3D plotting method by Akkineni *et al.*^[76] They mixed high concentration of alginate and 2–3 wt % of gellan gum. The addition of gellan gum prevents rapid swelling and thus improves the shape fidelity of printed scaffolds. Moreover, human mesenchymal stem cells on alginate/gellan gum composites displayed higher degree of cytocompatibility compared with pure alginate. The study explained that the improved initial cell attachment was related to the mechanical properties of hydrogels; stem cells preferred stiffer gels. Many researchers have highlighted that the cytocompatibility of gels is highly dependent on the mechanical properties of the hydrogel matrix.

In attempts to enhance the mechanical properties of hydrogel, two-component hydrogels consisting of a thermoresponsive polymer mixed with PEG or HAC were printed by 3D plotting^[77]. Starting materials were crosslinked by chemoselective reaction and extruded hydrogels showed mechanically stable hydrogels with a storage modulus of 9 kPa after 3 h. The hydrogel composite containing HAC exhibited high cell viability

of chondrocytes. Hong *et al.* developed 3D printed PEG/alginate hydrogel composite with stretchiness and toughness^[72]. Fabricated hydrogel composites had higher fracture energy than the value of cartilage and high cell viability after 7 days of culturing. The toughness of this hydrogel composite is attributed to the reversibly crosslinked calcium ions dissipating the mechanical energy and the covalently crosslinked PEG chains contributing to high elasticity.

Another method to tailor the mechanical strength is to co-print hydrogel with a stiffer polymer. Hyaluronic acid, the main ECM component of cartilage, with photi-reactive glycidyl methacrylate was printed as a porous scaffold by direct ink writing technique^[79]. The stiffness of scaffold increased as the contents of functionalized glycidyl methacrylate increased. When implanted in a porcine mandibular model, it showed good cell compatibility and enhanced tissue growth. Bakarich *et al.* blended alginate/poly(acrylamide) with acrylated urethane UV-curable adhesive (Emax 904) to fabricate biomimetic hydrogel composites^[70]. They adjusted the ratio of components by controlling the rates at which two materials stored in two separate syringes are dispensed into a single mixing nozzle (Figure 4A). As the volume content of Emax 904 increased, the tensile strength and elastic modulus also increased and this trend was in accordance with the rule of mixtures theory. Finally, they incorporated varying gradients into the printed scaffold to mimic living tissue such as tendon which links soft muscles to hard bone (Figure 4B).

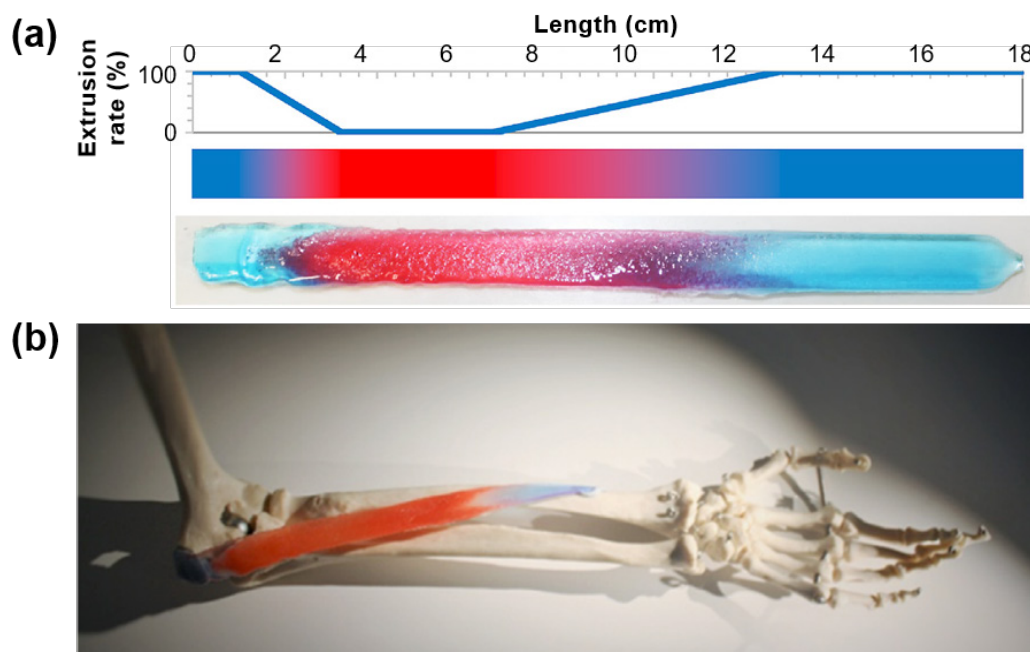


Figure 4. (A) The extrusion rate of Emax 904 as a function of the length and image of extruded gradient gel stained with red and blue dye. (B) Application of gradient gel which mimics the human tendon-muscle-tendon system in the place of pronator teres. (reproduced with permission from [70]. Copyright 2017, Elsevier Ltd).

A tunable degradation rate for hydrogels has also been thoroughly investigated so as to provide a tissue scaffold platform which gradually degrades over a few months as well as sufficient mechanical resistance. p(HPMA-lactate)/PEG hydrogel composites are printed with 3D plotting method by Censi *et al.*^[78] These hydrogel composites were crosslinked by thermal gelation and chemical crosslinks to stabilize the structure. Complete degradation of the printed scaffold was achieved in 190 days. In addition, the fabricated scaffolds showed similar mechanical characteristic with natural semi-flexible hydrogels such as collagen and displayed high chondrocytes viability after 1 and 3 days. Shie *et al.* also attempted to modify the degradation rate of hydrogels through a 3D printed polyurethane (PU)/HAc scaffold for use in cartilage tissue engineering^[82]. The water-based polyurethane (PU) with varying contents of HAc were printed by DLP process. The diametral tensile strength and elastic modulus of PU/HAc hydrogel composite are higher than those of pure PU hydrogel. After 28 days of degradation test, PU/HAc hydrogel composites with varying concentrations of HAc all exhibited similar degradation profiles. However, in the case of PU/HAc hydrogel composite scaffolds with over 2% of HAc, scaffolds showed ductile behavior even after 28 days of degradation. Meanwhile PU hydrogel and PU/1% HAc hydrogel demonstrated brittle behavior after degradation suggesting that the addition of HAc facilitated the stable degradation of hydrogel composite scaffolds.

3.2 Particle-reinforced Hydrogel Composites 3D Printing

Incorporation of micro- or nanoparticles into the hydrogel is widely used to enhance the mechanical and biological properties of pure hydrogels due to their low cost, ease of preparation, and isotropic strengthening behaviors^[11,12]. A particle-reinforced hydrogel composite is often formed from *ex situ* process in which the pre-formed or pre-purchased particles are dispersed into a hydrogel-forming liquid to be used for 3D printing (Figure 5A). This approach allows excellent control over the quantity of incorporated particles and greatly facilitates the study of optimal experiment conditions. Most particle-reinforced hydrogel composites are fabricated by this approach. For example, Fedorovich *et al.* used biphasic calcium phosphate (BCP) microparticles in the range of 106–212 μm for composite reinforcement and Matrigel or alginate as the hydrogel matrix. This particle-reinforced hydrogel composite was implanted in bone defects and used as an osteoinductive bone filler. Within 6 weeks of implantation, early osteogenesis of incorporated multi-potent stromal cells (MSCs) was induced. For 3D printing of particle-reinforced composites, nozzle sizes bigger than the microparticle size (420 μm internal diameter) were used and a 10-layer 3D scaffold ($10 \times 20 \times 1 \text{ mm}$) was fabricated *via* a 3D-bioplotter system. In the case of coarse microparticle-hydrogel composites, the mechanical enhancement is much lower compared to composites containing nano-sized particles, but it is easier to get a uniform particle distribution within the hydrogel through simple mixing due to its relatively low surface-to-volume

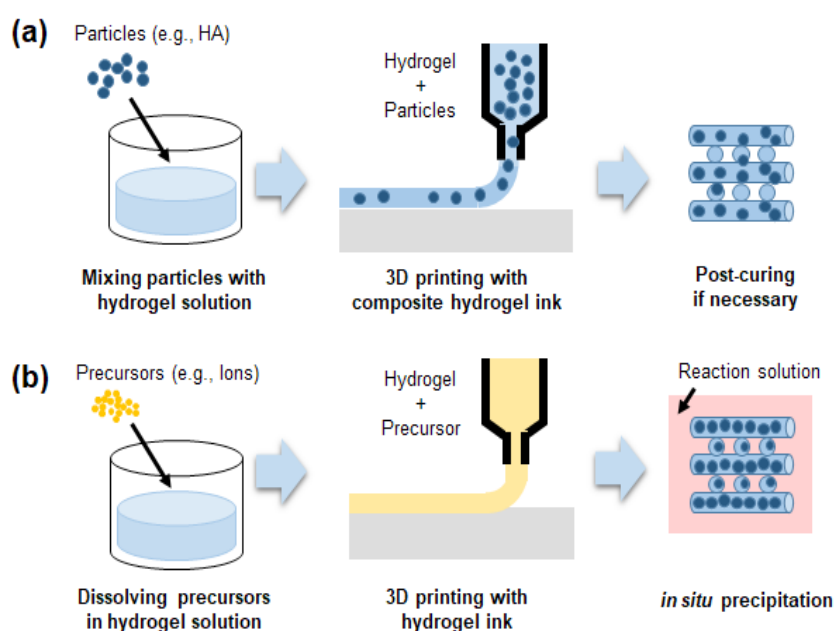


Figure 5. Schematic diagram of *ex-situ* and *in-situ* approaches for particle-reinforced hydrogel composite fabrication

ratio^[87].

Nanoparticle-reinforced hydrogels offer better mechanical and biological properties than microparticle-reinforced hydrogels. For example, Wüst *et al.* added HAp nanoparticles to a gelatin/alginate hydrogel system for bone tissue engineering applications, as shown in (Figure 6A). Gelatin provided the initial viscosity and mechanical stability required for the hydrogel ink to be printable due to its temperature-dependent physical crosslinking behavior. The long-term stability of the printed structure is achieved by the ionic crosslinking of alginate (Figure 6B). They fabricated simple structures using 3D-bioplotter printing which was modified with an in-house-fabricated heatable cartridge up to 40 °C to enhance the printability of composite hydrogels. By adding HAp nanoparticles (8% w/v), the Young's modulus was significantly increased with during the 3 day incubation period (Figure 6C). However, varying HAp concentrations from 0 to 4% did not induce a significant enhancement in the mechanical properties. Incorporation of HAp nanoparticles additionally led to radiopacity and thus visibility of constructed scaffolds under X-ray based medical detection, as shown in Figure 6D^[16]. Wang *et al.* investigated the effect of bioglass nanoparticles, with the size of 55 nm, on encapsulated SaOS-2 cells. An alginate/gelatin/SaOS-2 cell suspension supplemented with bioglass nanoparticles was placed into sterile 3D-bioplotter printing cartridges, and printed into a hydrogel scaffold (13 × 13 × 1.5 mm). During the incubation periods of 3 and 5 days,

bioglass-reinforced alginate/gelatin hydrogel composites showed significant enhancement of proliferation and mineralization of bioprinted SaOS-2 cells^[83].

In spite of the superior mechanical and biological performances of inorganic particles, the major problem of the *ex situ* incorporation approach is the limit on the maximum amount of particles that can be added to the hydrogel; introducing nanoparticles into the hydrogel rendered the printing ink more viscous and harder to print in the desired way. In previous studies, maximal nanoparticle inclusion to ensure proper printability and structural accuracy was found to be limited to 10%. Nearing the 10% nanoparticle inclusion, slight irregular filament shape and ununiform size distribution were induced^[16]. Skardal *et al.* introduced gold nanoparticles (AuNPs) into semi-synthetic extracellular matrix (sECM) hydrogel composites which can generate dynamic crosslinking between intra-gel and inter-gel during and after printing. In particular, 2.5% w/v of 25 nm gold nanoparticle provided enough mechanical stability to support multilayered 3D structures by the physical reinforcement effect, and after 60 min of printing, adjacent filaments were completely joined by slow rate of inter-filament crosslinking between AuNP and sECM hydrogel^[86]. This dynamically crosslinked AuNP-sECM hydrogel may provide new strategies in the *ex situ* particle incorporation approach for the 3D printing hydrogel composite system.

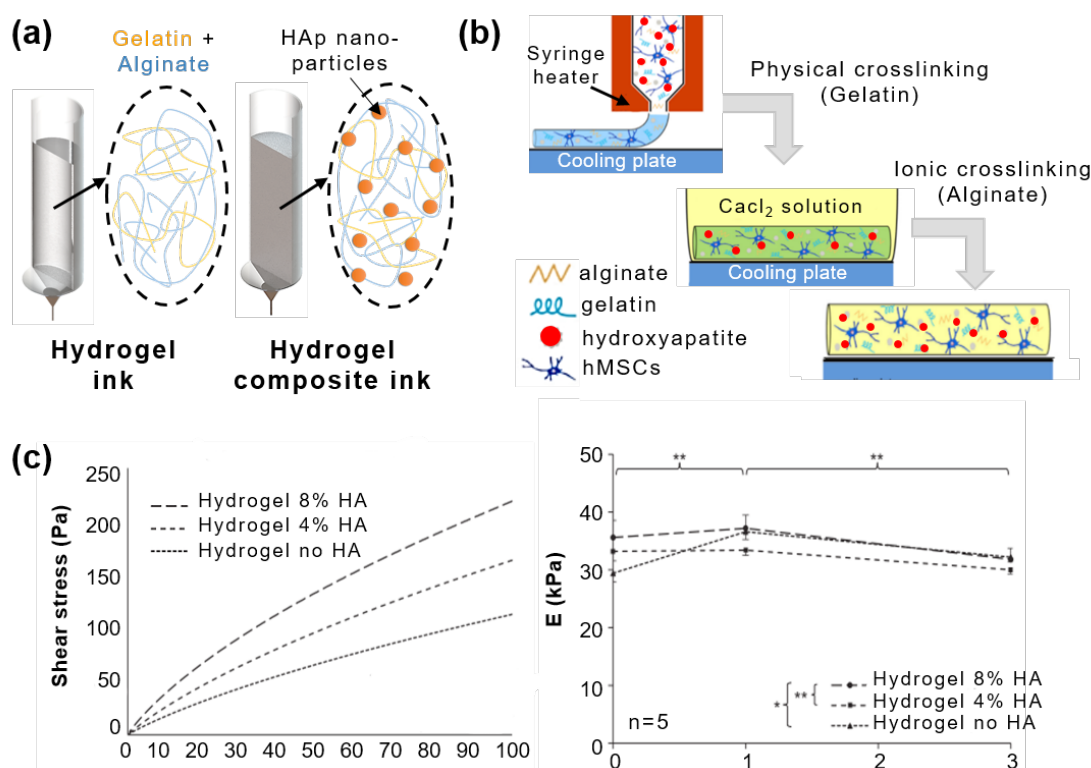


Figure 6. Schematic images of (A) gelatin/alginate hydrogel and its composite with Hap nanoparticles and (B) two-step hydrogel gelation process. (C) Rheological properties of hydrogel composites (left: shear stress plotted over a shear rate, right: elastic modulus over 3 days). (D) Optical microscopic and micro-CT images of 3D printed patterns. (reproduced with permission from [16]. Copyright 2014, Elsevier Ltd).

The *in situ* incorporation of particles into hydrogel scaffolds during and/or after 3D printing is more-effective approach than the *ex situ* method for achieving uniform distribution and high loadings, because post-loaded particles do not hinder the printing process (Figure 5B). Jeong *et al.* proposed a great potential of *in situ* precipitation process for high- and uniform-loading capacity with minimal agglomeration into a polymer matrix. Precipitated calcium phosphate (CaP) nanoparticles with 200–350 nm were easily formed and incorporated from calcium chloride and phosphoric acid mixed solutions. Compared with same concentration of pre-mixed CaP nanoparticles, precipitated HAc-CaP composite hydrogels exhibited homogeneous distribution and approximately five times higher storage moduli values. In addition, mechanical properties were continuously increased by increasing concentration of precipitated CaP up to 40 wt%^[15]. Very recently, Egorov *et al.* combined *in situ* mineralization with 3D printing in which calcium chloride and ammonium hydrogen phosphate solutions were mixed with sodium alginate slurry and then 3D-biplotter printing was employed to fabricate a cubic-shaped 3D composite structure (8 × 8 × 5 mm). The compressive strength of composite hydrogels were gradually increased from 0.4 to 1.0 MPa with increasing concentration of precipitated CaP up to 2.0 wt%. However, overall mechanical properties of 3D printed scaffold were relatively low due to the weak bonding between filaments, which is a major limitation of the *in situ* particle incorporation approach for composite hydrogel systems^[99].

3.3 Fiber-reinforced Hydrogel Composites 3D Printing

Fiber reinforcements can also improve mechanical properties of hydrogel matrix in which the fiber contents and its distribution inside its matrix determine mechanical properties such as stiffness and strength of composites^[92–95]. In the case of common 3D printing systems, short fiber reinforcements are the most commonly used due to its easy processing procedure at low cost. The fibers can be directly incorporated into the hydrogel matrix *via* simple mixing and transferred into the syringe for printing. Gladman *et al.* proposed stiff cellulose fibrils as a short fiber reinforcement and printed cellulose-acrylamide composite hydrogel 3D structures. For ensuring smooth, clog-free print behavior of composite ink, the maximum concentration of nanofibrillated cellulose inside a soft acrylamide matrix should not exceed 0.8 wt%, which was then transferred into the 3D-biplotter cartridge and injected through stainless steel commercial nozzles of varying diameters. During the printing process, short fibers inside the composite ink undergo shearing forces due to the small nozzle size and orientate themselves along the printing direction, as shown in Figure 7A. This in turn induces anisotropic mechanical properties of printed filaments such as anisotropic stiffness and swelling behaviors^[92].

In the case of long and continuous fiber-reinforced hydrogel systems, research has shown substantially improved mechanical performances due to the continuous fiber-hydrogel matrix interactions as opposed to disconnected interactions in short-fiber-reinforced hydrogels. As such, the load transmittance from the matrix to each fiber also becomes more continuous. However, in spite of its outstanding performance, the most challenging issue for applying this composite system to the 3D printing process are practical ways to achieve an uniform distribution and intended alignment of continuous fibers within the hydrogel matrix. Narayanan *et al.* tried to fabricate alginate-nanofiber bioink for 3D-bioprinting which could provide protection for encapsulated cells during the digitally driven fabrication process^[93]. To prepare the composite hydrogel, pre-fabricated portions of PLA nanofiber was mixed with alginate (ratio 1:5, w/w), and agitated in a vortex mixer, and finally sonicated for 2 hours. Despite all these efforts, continuous PLA nanofibers were aggregated and poorly distributed within hydrogel matrix, which is mainly attributed to the strong van der Waal's attraction between the sub-micron scaled aggregated fibers (Figure 7B). In this paper, they could not prove there were any mechanical enhancement of nanofiber-reinforced composite hydrogels, but the nanofiber-reinforced bioink showed better cell proliferation and metabolic activity levels of human adipose-derived stem cells (hASC) within printed 3D structure that were encapsulated with cells^[93].

Agrawal *et al.* approached this issue from a different angle. To build continuous fiber-PEG composite scaffold, elastic polyurethane (PU) fibers are printed first to form a “log-pile” structure, and then fabricated continuous fibers were impregnated with the PEG gel. The PU polymer solution was placed into a pressure-driven syringe fitted with a 100 μm needle, and mounted on the dispensing 3D printing system. The entire printing process was performed under water to form a continuous elastic micro fiber rapidly though solvent exchange. As with 24 wt% continuous fibers, the elastic modulus of composites were two-times higher, and the maximum strain-to-break ratio was greatly improved compared to that of pure hydrogels^[94]. Bakarich *et al.* developed a more advanced technique for fiber-reinforced hydrogel composite system using a one-step process^[95]. The previous approach requires at least a two-step fabrication process involving the 3D printing of continuous fiber scaffold structure followed by immersion of the scaffold into a hydrogel precursor solution, and crosslinking. However, recent development of UV curable material and light system of 3D printing have made it possible to fabricate fiber reinforced hydrogel composites using a one-step 3D-biplotter process. This composite was printed by selectively patterning a combination of two different UV curable inks: one is alginate/acrylamide gel solution for the matrix, and the other is adhesive epoxy

resin (Emax 904 Gel-SC) for the reinforcement. Composite digital models of hydrogel matrix and fiber reinforcement were constructed using computer-aided designs and the printing path was also precisely generated by the software. For evaluating mechanical properties of fiber reinforced composite hydrogel, a dog-bone shaped tensile strength specimen with uniaxial oriented continuous epoxy fiber was successfully fabricated as shown in (Figure 7C). The printed composite hydrogels showed a combination of properties in between pure hydrogel and epoxy resin, and its elastic modulus, failure strength, failure strain properties were gradually increased by increasing the relative volume of epoxy fibers. A noticeable finding in this study is that there is no limitation of fiber

reinforcement amount inside the hydrogel matrix. They showed extremely wide range of fiber volume fraction from 0 to 100% inside alginate hydrogel matrix, and the bond between the hydrogel and fiber is stronger than pure hydrogel so that under the applied stress, matrix and fibers were equally deformed without any interfacial slipping between them. The reinforced fibers experience a greater stress than the hydrogel matrix^[95]. So far, these studies have only demonstrated the feasibility of 3D printing for fiber-reinforced composite hydrogel, but the further development of composite 3D printing techniques is crucial before they can be applied to various tissue engineering applications such as biofabrication of skin, muscle, tendons, and cartilage in the near future.

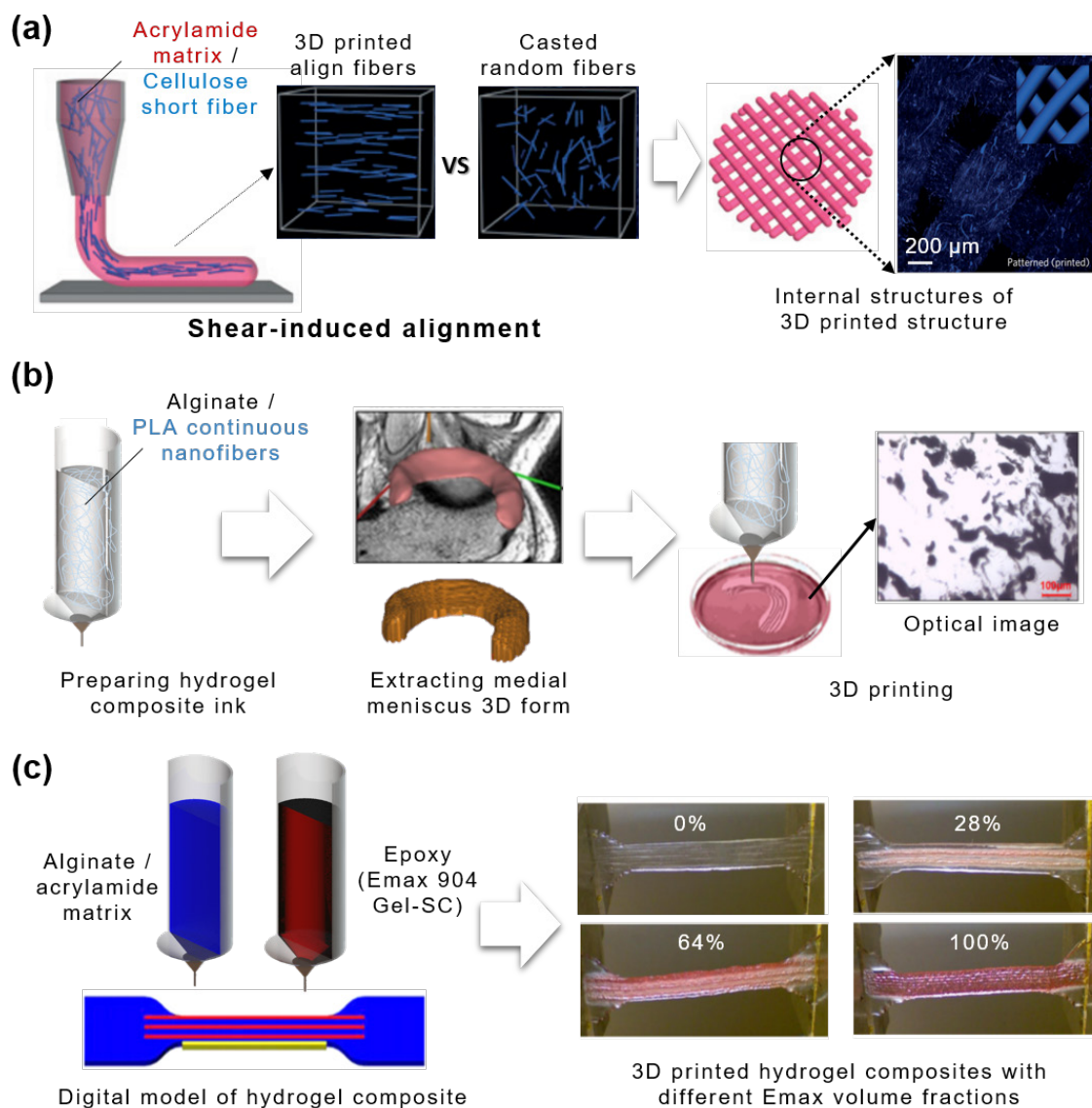


Figure 7. (A) Schematic images of cellulose short fiber alignment during the 3D printing (reproduced with permission from [92]. Copyright 2016, Macmillan Ltd). (B) Overview of 3D printing process of PLA nanofiber-alginate hydrogel composite, and its internal structure (reproduced with permission from [93]. Copyright 2016, ACS Publications). (C) Schematic image of the fabrication of hydrogel composite tensile specimen, and its photographs with different Emax volume fractions (reproduced with permission from [95]. Copyright 2014, ACS Publications).

3.4 Anisotropic Filler-Reinforced Hydrogel Composites 3D Printing

Nanoclay is a nanoparticle which is composed of layered hydrous silicate. It has been used in a wide range of applications such as pharmacy, paints, cosmetics as well as catalysis owing to their good surface properties and excellent rheology controllability. Depending on the type of clay, each layer consists of two or more sheets of either $(\text{AlO}_3(\text{OH}))_3$ octahedra or $(\text{SiO}_4)_4$ -tetrahedra. Nanoclays are classified into several classes such as Laponite, montmorillonite, bentonite, nontronite, saponite, kaolinite, hectorite, and halloysite by their geometrical shape and chemical composition which can affect biocompatibility. Rawat *et al.* investigated the cytotoxicity and antimicrobial properties of various shape and concentration of nanoclays^[100]. They prepared Laponite with an aspect ratio of 25:1 and montmorillonite (MMT) with an aspect ratio of 300:1. The cytotoxicity and antimicrobial properties of both nanoclays with various concentration from 0.00005 $\mu\text{g}/\text{mL}$ to 0.0125 $\mu\text{g}/\text{mL}$ were assessed by eukaryotes-human embryonic kidney (HEK), and cervical cancer SiHa cell and Kirby-Bauer protocol method, respectively. Laponite exhibited good antimicrobial properties, while MMT showed better cytotoxicity. Their explanation behind this finding is due to the difference in charge density and anisotropy of the clays. Modification of nanoclays as organic-inorganic hybrid nanomaterials have potentials for use as rheological modifiers, gas absorbents and drug delivery carriers in customizing polymer composites.

Laponite, a synthetic magnesium silicate, is well known as a nano biofiller in cosmetics. The potential use of Laponite as tissue engineering constructs has been discussed because they enhance cell spreading and promote osteogenesis. The crystal structure of Laponite is a disc-shaped layered magnesium silicate with a particle size of approximately 25 nm in diameter and 1 nm in thickness as shown in (Figure 8A). These ultrathin structures with a high degree of anisotropy and functionality enhance their surface interactions. In addition, Laponite is negatively charged on its face and positively on the rim thus undergoes self-assembly through electrostatic interactions to form a shear thinning gel state with a “house-of-cards structure” (Figure 8B)^[101]. Therefore, many studies have been carried out on blending Laponite with polymers for improving mechanical and biological properties. Hydrogels with poor mechanical properties can yield these properties by forming strong interaction between chains of hydrogel and monodispersed Laponite. Su *et al.* fabricated silk fibroin hydrogel composites with Laponite for bone defect repair application^[102]. As the concentration of Laponite increased from 0 to 5%, rheological properties of hydrogel composites increased from 30 to 200 kPa. Osteoblasts cell proliferation and differentiation also increased with the addition of Laponite. Injectable hydrogel nanocomposite was investigated by combining Laponite and dopamine-

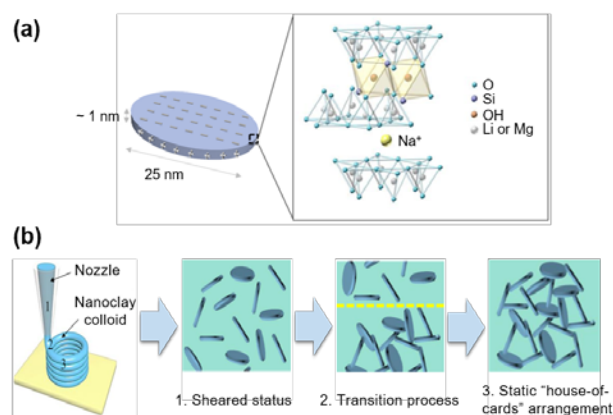


Figure 8. (A) The structure and composition of Laponite nanoclay as an anisotropic filler and (B) “house-of-cards” mechanism of self-assembling printed hydrogels including Laponite. (reproduced with permission from [96]. Copyright 2017, ACS Publications).

modified four-armed poly(ethylene glycol) (PEG-D4) Liu *et al.*^[103] The introduction of Laponite did not change the degradability and cytocompatibility of PEG-D4. However, the curing time, mechanical and adhesive properties were significantly increased. Consequently, PEG-D4/Laponite hydrogel nanocomposites minimized inflammatory response and improved cellular infiltration in vivo as compared to Laponite-free specimens.

Recently, a variety of Laponite incorporated hydrogel composites are 3D-printed for hard tissue engineering. Jin *et al.* proposed a direct hydrogel printing approach without any supporting bath by using self-supporting nanoclay^[96]. Laponite RD and XLG were mixed with three types of hydrogels including poly(ethylene glycol) diacrylate (PEGDA), alginate, and gelatin. Each prepared composites were extruded by direct ink writing with appropriate crosslinking methods, respectively. Laponite-incorporated hydrogels were readily printed through a nozzle and solidified after extrusion in the air. The addition of Laponite improved the mechanical properties of extruded scaffolds and also adjusted the degradation rates. The elastic modulus of PEGDA-Laponite, alginate-Laponite, and gelatin-Laponite scaffolds increased 1.9, 7.4 and 3.3-fold than each pure hydrogels without Laponite, respectively. The cytocompatibility of PEGDA-Laponite was confirmed by fibroblast cell adhesion and proliferation.

Zhai *et al.* reported that the physical crosslinking of hydrogel chain-clay coupled with hydrogen bonding remarkably increased the mechanical performance of hydrogel scaffolds^[97]. N-acryloyl glycinamide (NAGA) was dissolved in deionized water with varying concentrations from 10 to 30%, and then mixed with different quantities of Laponite XLG. The mixed solutions were extruded by 3D plotting method and printed specimens were cured in a cross-link oven. Fabricated PNAGA-Clay scaffolds showed homogeneous structures and the mechanical properties of

scaffolds in tension and compression tests significantly increased with the addition of Laponite XLG. The release of silicon and magnesium ions from Laponite XLG promoted the proliferation and differentiation of primary rat osteoblast (ROB) cells. PNAGA-clay hydrogel scaffolds implanted in tibia defects of rats effectively induced new bone formation.

The possibilities of bioprinting and growth factor delivery of hydrogel-nanoclay composites were verified by Ahlfeld *et al.*^[98] Laponite XLG was blended with various compositions of alginate-methylcellulose hydrogels. The pastes were printed by 3D plotting method and incubated in CaCl₂ solution. Human telomerase reverse transcriptase-mesenchymal stem cells (hTERT-MSK) were mixed with prepared hydrogel composite pastes before printing for cell plotting. Bovine serum albumin (BSA) and vascular endothelial growth factor (VEGF) were also loaded in advance into hydrogel composite pastes for release tests. Scaffolds were well-extruded with high shape fidelity by the addition of nanoclay. After 21 days, the printed hTERT-MSK showed cell viability of approximately 70%–75%. Continuous release of BSA and VEGF, from the hydrogel composite scaffolds, was observed even after 21 and 7 days, respectively.

4. Applications and Challenges

4.1 Hard Tissue Engineering Application

3D printing technologies have been used by medical professionals in a wide range of applications. Initially, only visual models and functional prototypes were fabricated by 3D printers. However, with improved accuracy of 3D printing process as well as the development of medical imaging, or radiology equipment such as magnetic resonance imaging (MRI) and computed tomography (CT), 3D printing technologies can now be used to produce tissues or organs which are directly implanted into the human body. The customized implantable scaffolds for patients are designed to better fit the affected site using reconstructed MRI and CT images. In particular, porous scaffolds which induce cell infiltration and proliferation are more easily produced by 3D printers as compared to other traditional processes such as subtractive manufacturing.

As mentioned before, pure hydrogels have poor mechanical properties. Therefore, in order to match the mechanical properties of tissues or organs, the integration other materials to form hydrogel composites is essential. Hard tissue engineering such as bone regeneration is one of biomedical fields that require these composites (Figure 9). The material needs sufficient strength and elastic modulus as well as good biocompatibility. HAp, the main component of bone, is a promising reinforcement that can be used to improve these conditions. Various sizes of HAp particles from nano to micro scale were

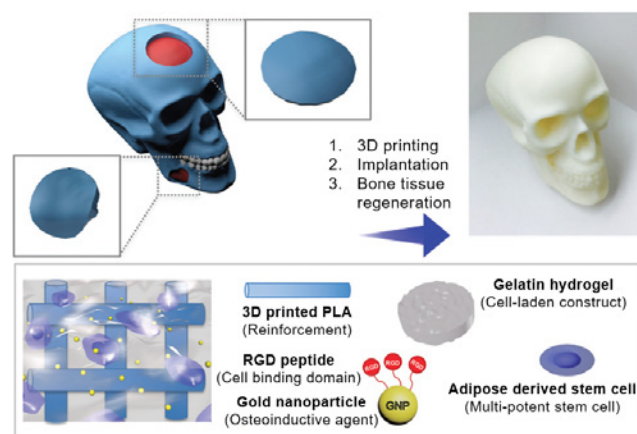


Figure 9. Customized bone defect regeneration using a extruded PLA and gelatin hydrogel composite with incorporated human adipose derived stem cells and gold nanoparticles (reproduced with permission from [89]. Copyright 2017, Royal society of chemistry).

dispersed in hydrogels and printed as bone substitute scaffolds. Demirtas *et al.* printed chitosan-HA hydrogels using a 3D plotting method and compared them with alginate-HAp hydrogels^[104]. With the addition of about 180 nm HAp particles, elastic modulus of alginate-HAp hydrogels and chitosan-HAp hydrogels increased approximately 3-and-5 fold compare to pure alginate and chitosan hydrogels. The hydrogels loaded with pre-osteoblast cells, chitosan-HAp hydrogels showed higher expression of osteogenic differentiation marker on day 21 when compared with other hydrogels. Other calcium phosphate materials including bicalcium phosphate (BCP) and tricalcium phosphate (TCP) are also proposed as hydrogel fillers for bone tissue engineering. Diogo *et al.* mixed alginate with beta-TCP and extruded by 3D plotter^[105]. Various composition of beta-TCP/alginate of 50/50% (w/w), 30/70% (w/w) and 20/80% (w/w) were evaluated. As the beta-TCP contents in alginate matrix increased, the accuracy of printing increased due to increase in the viscosity of hydrogel composites. 50/50 beta-TCP/alginate scaffolds had the highest compression strength and Young's modulus and these values are higher than those of trabecular bones. Furthermore, biological test using osteoblast cells suggested that 50/50 beta-TCP/alginate scaffolds have potential as composite scaffolds in bone regeneration applications.

Similarly, studies were also carried out on bioglass incorporated hydrogel composites^[106]. 3D printed collagen/alginate was coated with silica by soaking the scaffolds in tetraethyl orthosilicate (TEOS) with various concentrations^[107]. The scaffolds were more mineralized in simulated body fluid solution as the fractions of silica in collagen/alginate scaffolds increased. The degradation rate of silica coated collagen/alginate scaffolds was significantly reduced while the elastic modulus of silica coated collagen/

alginate scaffolds increased. *In vitro* cellular response using pre-osteoblast cells exhibited that silica coated collagen/alginate scaffolds had higher value of proliferation and gene expression than pure hydrogel scaffolds. Wang et al. added various kinds of bioglass including polyphosphate (polyP), polyP*Ca²⁺-complex, silica, and biosilica produced by sol-gel method in to alginate/gelatin/SaOS-2 bone cell hydrogels composites^[108]. Each of the mixed pastes were extruded by 3D bioplotter and results showed that the added polyP and biosilica increased the proliferation and mineralization of bone cells.

4.2 Soft Tissue Engineering Application

Cartilage is a kind of soft tissue, which is a complex structure composed of interstitial fluid, collagen and chondrocytes. Cartilage tissue engineering has been widely investigated because the injured cartilage does not heal or regenerate by itself^[109]. Hydrogels are excellent alternatives for use in cartilage engineering since they are highly hydrated with a cross-linked architecture that can be filled with cells. These hydrogels scaffolds can be easily prepared by 3D printing but their poor mechanical stability remains a big challenge. Therefore, many researchers have put in efforts to overcome this limitation by mixing pure hydrogels and fillers.

Bartnikowski fabricated multi-layered hydrogel composites comprising functionalized gelatin methacrylamide

(GelMA) or GelMA with hyaluronic acid methacrylate (HAMA) on pure alginate or alginate/hydroxyapatite (HAp) composites by 3D plotting^[110]. Incorporation of hydroxyapatite increased the elastic modulus of printed hydrogel composites and HAMA in GelMA hydrogels improved chondrogenesis. The polycaprolactone (PCL) and alginate were printed layer-by-layer with a multihed deposition system as shown in (Figure 10A)^[111]. These hydrogel composites combined chondrocyte cells and transforming growth factor beta (TGF-beta) to mimic the properties of cartilage. PCL/alginate scaffolds with TGF-beta showed higher cartilaginous ECM formation. *In vivo* test using dorsal subcutaneous zone of nude mouse showed that the amounts of collagen fibers and cartilaginous tissue formation of chondrocyte encapsulated PCL/alginate scaffolds with TGF-beta were higher than other control hydrogels. PCL was also used as composite material for cartilage tissue engineering applications^[112]. Electrospun PCL and fibrin/collagen hydrogel containing chondrocytes were fabricated layer by layer by hybrid inkjet printing/electrospinning system. The printed hybrid composite scaffolds showed higher tensile properties compared with each of the PCL and fibrin/collagen hydrogels alone. Printed chondrocyte cells maintained more than 80% of viability *in vitro* and large amounts of collagen and glycosaminoglycans which are similar to elastic cartilage were produced *in vivo*. In order to fabricate tough hydrogels for cartilage tissue engineering applications, agar was combined with alginate by Wei *et*

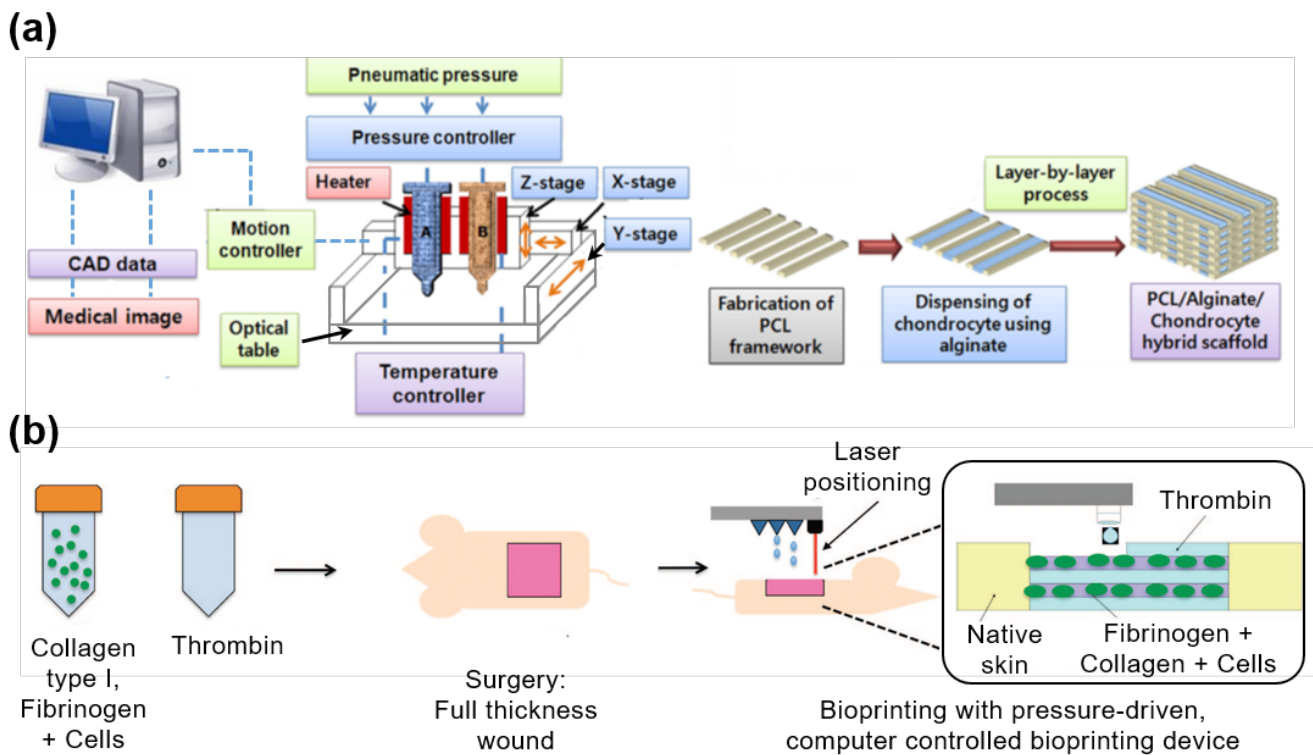


Figure 10. Schematics of (A) the 3D printing process of chondrocyte-incorporated alginate-PCL hybrid scaffold for cartilage application (reproduced with permission from [111]. Copyright 2013, John Wiley & Sons, Ltd) and (B) the direct bioprinting process of collagen-fibrinogen with stem cells onto skin wound of rat (reproduced with permission from [116]. Copyright 2012, AlphaMed Press).

al.^[113] The addition of alginate not only improved the hydrogel viscosity and shape fidelity, but also increased the tensile strength and toughness of hydrogels.

The skin is the largest organ that covers the human body and it plays an important role in regulating temperature, controlling evaporation as well as protecting from pathogens and external environment. It is a complex structure with three sequential layers including epidermis which is the outer layer, dermis that is permeated by a complex nervous and blood vessel, and hypodermis consisting of subcutaneous tissue^[114]. Therefore, in skin tissue engineering, many researchers tried to substitute this complex and important organs with artificial skin grafts such as hydrogels for curing skin wounds and diseases^[115]. With recent advances in hydrogel printing technique which moved from 2D to 3D printing allow more flexibility in controlling the micro/nano level structure. Moreover, studies are focused on 3D printing hydrogel composites to functionalize hydrogel scaffolds that are closely mimicking real skin tissue.

Skardal *et al.* investigated the possibility of skin regeneration of mouse skin wound by printed amniotic fluid-derived stem (AFS) cells incorporated hydrogels^[116]. They used fibrinogen/collagen mixed with 50:50 volume ratio as hydrogel composites and hydrogel composites including AFS cells and mesenchymal stem cells (MSCs). Fibrinogen/collagen hydrogel composites with cells and thrombin were directly printed on the skin wound of nude mouse layer-by-layer by inkjet 3D printer (Figure 10B). The wounds treated by composite with AFS cell and MSC cells showed better wound closure and re-epithelialization results up to 14 days than those of fibrin/collagen gel up to 14 days with increased vessel density and enlarged capillary diameters.

Chitosan and graphene were used as hydrogel composite materials for tissue engineering^[84,117]. Chitosan has been used in artificial skin and wound dressing with its similarity in hyaluronic acid content and glycosaminoglycans in joints^[118]. The limitations of chitosan are its poor mechanical properties and slow gelation rate. In Sayyar's studies, chitosan or methacrylated chitosan (ChiMA) were mixed with various contents of graphene and extruded by modified computer numerical control (CNC) machine. Both graphene/chitosan and graphene/ChiMA hydrogels showed tunable swelling properties and good biocompatibility which was confirmed with fibroblast cell adhesion and proliferation test on the hydrogel composites. As the contents of graphene in chitosan or ChiMA increased, tensile strength and conductivity remarkably increased.

For 3D printing of soft tissue engineering scaffolds, cell-laden bioinks are often used. Despite of numerous advantages of bioprinting, the harsh conditions imposed by the printing process have led to the rise of new challenges regarding the processing of sensitive cells and biomolecules due to 3D printing conditions required by different types of 3D printers and the chosen bioink^[119]. In thermal, laser

and piezoelectric inkjet, cell damage mainly results from the thermal heating during the printing process, whereas in extrusion bioprinting, compression forces and shear stresses generated during the printing causes damage to cells^[120]. On the other hand, biocompatible hydrogels widely used for matrix materials of cell-laden bioinks or supporting materials of printed cells require solidification strategies, *e.g.*, photo-crosslinking, *in situ* chemical crosslinking, physical crosslinking or shear-thinning^[121-124]. Integration of those solidification methods into bioinks is challenging, particularly in case of cell-laden hydrogel bioinks where the hydrogel gelation process should minimize the potential damage of encapsulated cells^[121-123,125,126]. Particularly, UV-based photopolymerization reactions of bioactive hydrogels (*e.g.*, gelatin, collagen, chitosan) are commonly coupled with bioprinting, employed either during the printing process^[127] or after the deposition of bioinks^[39] to produce stable 3D hydrogels with intricate architectures for cell encapsulation. However, the deleterious effects of UV light irradiation and cytotoxicity of radicals generated by photoinitiators lead to a decrease in cell viability and ultimately DNA damage^[128].

4.3 Vascular Application

Fabrication of vascular system is one of the main challenges in 3D printing, because isolated cells cannot live in spaces of less than 3 mm³ of volume^[129]. Vascular channels transport oxygen, growth factors and nutrients and remove the waste solutions for living cells. Therefore, well-designed blood vessel tree of capillaries and microvessels are required for operating large tissues or organs. Moreover, sufficient mechanical properties are also needed for vascular tissue engineering to tolerate physiological pressures and surgical connections.

To achieve this goal, double-nozzle assembling method was adapted to 3D-print vascular for liver by Li's group^[130]. Li fabricated gelatin/alginate/chitosan (GAC) hydrogel composites combined with adipose-derived stromal cells (ADSC) and printed them to form vascular networks. Gelatin/alginate/ fibrinogen (GAF) hydrogel was also combined with hepatocytes and placed around the printed ADSC/GAC hydrogel composites to mimic anatomical liver structure. The vascular channels were crosslinked with thrombin, CaCl₂, Na₅P₃O₁₀ and glutaraldehyde and were well maintained for more than 2 weeks. Printed ADCSs differentiated into mature endothelial cells and the albumin secretion value of the hepatocytes increased after 2 weeks of culturing. In a similar way, the production of perfusable vascular systems with highly ordered arrangements was achieved by a multiple coaxial nozzle as shown in (Figure 11A)^[131]. They mixed gelatin methacryloyl (GelMA) and 4-arm poly(ethylene glycol)-tetra-acrylate (PEGTA) for fixing the morphologies of the constructs permanently and sodium alginate for maintaining the shape by fast

ionic crosslinking. The perfusable structures with multiple layers and various diameters were formed by coaxial nozzle systems in a one-step process. The rheological and mechanical properties of the printed hydrogel composites were tunable by PEGTA and endothelial and mesenchymal stem cells incorporated hydrogel composites also showed favorable biological responses which demonstrated the formation of vessels resembling early maturation of the native vasculature.

PEG derivatives were used as crosslinkers to develop bioartificial vessel-like grafts. Different four-armed polyethylene glycol (PEG) derivatives called TetraPEG8 and TetraPEG13 were converted to tetra-acrylate derivatives (TetraPACs) and these were co-crosslinked with hyaluronan acid and gelatin hydrogels into synthetic extracellular matrices (sECMs) by Skardal *et al.* (Figure 11C)^[132]. The crosslinked hydrogel composites showed improved rheological properties which are more suitable for bioprinting when compared with sECM hydrogels crosslinked with PEGDA. Bioprinted hydrogel composites containing NIH3T3, HepG2 C3A, and Int407 cells exhibited microcapillary tube structure with cells viability up to 4 weeks.

Dolati proposed bioprintable vascular conduits reinforced by carbon nanotubes^[133]. Multiwalled carbon nanotubes (MWCNTs) were dispersed in alginate hydrogels and human coronary artery smooth muscle cells (HCASMCs) encapsulated hydrogel composites were extruded by coaxial nozzle. As contents of MWCNTs increased, the mechanical properties of hydrogel composites increased. However, in long-term biological responses, MWCNT-added hydrogel

composites induced cell toxicity.

4.4 4D printing

The applications of the hydrogel composite systems are not only limited to mechanical strengthening or biological performance. They are also valuable model systems for stimuli-responsive smart materials, also known as 4D printing. 4D printing involves materials that are responsive to external stimuli such as electricity, light, ions, temperature, and water, such that the pre-printed 3D configuration changes over time^[92,134–138].

In general, shape memory polymers (SMPs) are popularly used for the 4D printing which have permanent shape by a cross-linked polymer network, and can be deformed into a temporary shape *via* reversible interactions between the networks. When exposed to external stimuli, the material can recover its original shape. However, most SMPs only possess 3D printability with laser-based printing systems such as Polyjet or SLA 3D printing^[135,136]. Therefore, there are severe limitations on the choice of material and function for tissue engineering applications.

In the case of hydrogel composite, they have a great potential as a platform technology to extend material choice for 4D printing with their highly tunable functionalities. For example, it is possible to utilize hydrogel composites for water-activated 4D printing. In general, reinforcements such as inorganic particles or fillers do not or exhibit less swelling behavior in water as compared to hydrogels (Figure 12A). The orientation or distribution of reinforcements within the hydrogel composite generates controllable

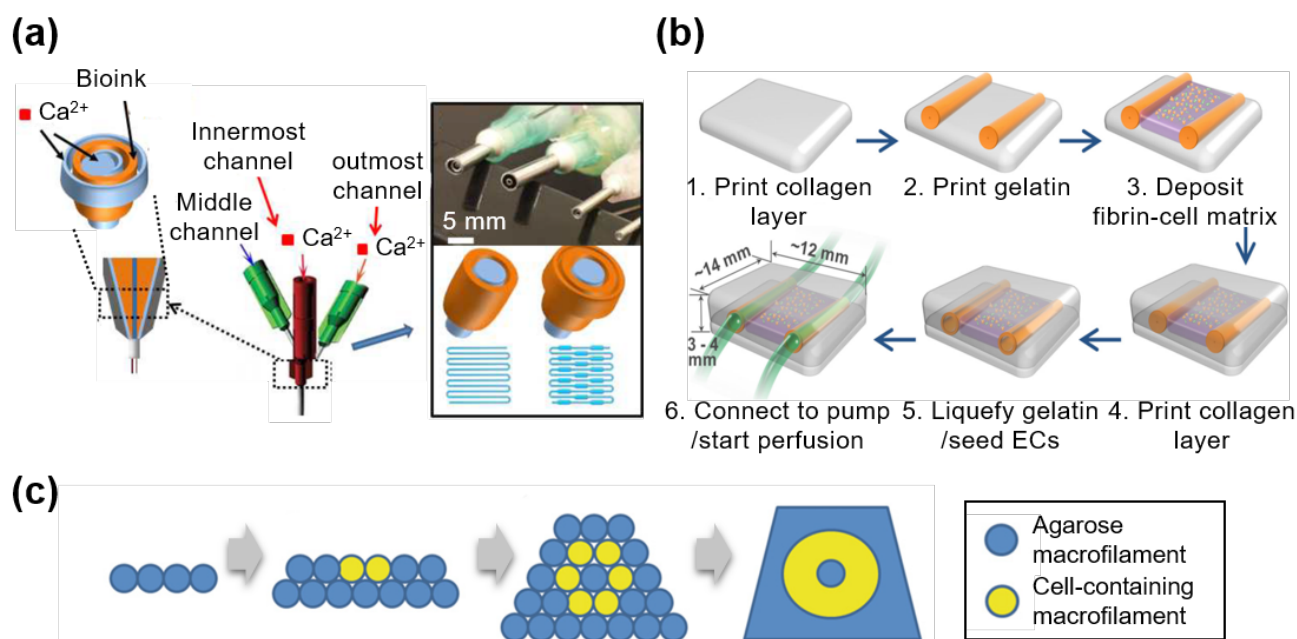


Figure 11. Various strategies of constructing vascular system (A) using a multiple coaxial nozzle with alginate, GelMA, and 4-arm PEGTA (reproduced with permission from [131]. Copyright 2016, Elsevier Ltd), (B) bioprinting layer-by-layer with collagen, fibrin-cell mixture, and sacrificial gelatin, (reproduced with permission from [140]. Copyright 2017, Springer International Publishing AG.) and (C) by stacking hydrogel macrofilaments to form a cellularized tubular structure (reproduced with permission from [132]. Copyright 2010, Elsevier Ltd).

anisotropic swelling and allows precise control over the printed structure's curvature (Figure 12B)^[92]. Thus, by utilizing the swelling behaviors of hydrogel composite structures, bio-origami hydrogel scaffolds can be developed with self-folding behavior under the appropriate external stimuli, which can greatly contribute to the fabrication of functional 3D tissues.

4D printing technique is also attractive for drug delivery systems in which precise control over the shape of the carrier is desirable to release drugs or cells in a programmable manner. For example, in the case of mucoadhesive drug delivery systems, hydrogel bilayer structures composed of two differentially swelling layers can induce self-folding property, which makes it more likely to stick to the mucus tissue. The less or non-swelling layer acts as a diffusion barrier and incorporated drugs can be released unidirectionally towards the adhered tissues, which minimizes drug leakage and enhances drug delivery efficiency^[134,137].

Until now, existing self-assembly or self-folding 4D printing systems are limited to macroscale deformations, which restricts the precise spatial manipulation of 4D-printed structures. In addition, most responsive materials only respond to one type of external stimulus. For tissue engineering applications, printed scaffolds need to adapt to complicated microenvironments of within the human body^[134,138]. Therefore, the future of 4D printing requires a stronger focus on microscale controllability over the shape, orientation, or biocompatibility of printed structures. This can be achieved by improving printing resolution and material design in response to multiple physiological signals.

5. Conclusion and Future Outlook

In this paper, the pros and cons of utilizing hydrogel composite materials as printing ink in 3D printing systems has been thoroughly discussed. This information will be useful for selecting the printing method and appropriate materials for the desired biological performances. The

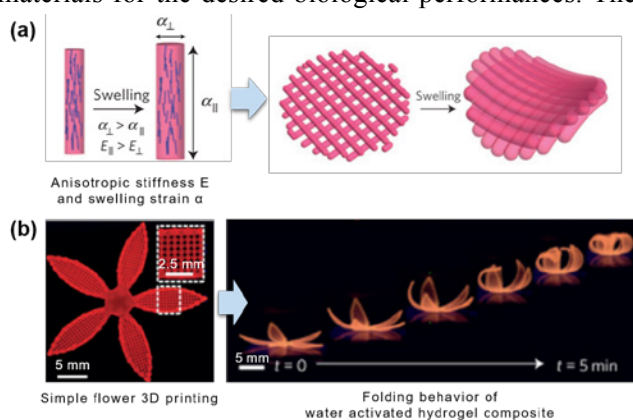


Figure 12. (A) Schematic images of cellulose fibrils alignment-induced anisotropic stiffness E and swelling strain α , and (B) its water-activated 4D printing effect. (reproduced with permission from [92]. Copyright 2016, Macmillan Ltd).

recent developments of 3D printing system tend to bring the hydrogel-based tissue engineering on the next level. In recent years, hydrogel composite 3D printing techniques have gone through tremendous technological improvements in the form of material design and printing system optimizations. However, there are still several critical issues and problems that needs to be addressed.

First of all, hydrogel cross-linking methods that are available in 3D printing systems are severely limited. For the construction of stable 3D structures, hydrogel materials which crosslink rapidly is essential to support each printing layer before they collapse under their own weight, and until now, only photo- and ionic-crosslinking strategies are applicable for 3D printing due to their high crosslinking efficiency. However, the limited materials and printing systems could not meet the stringent requirements demanded by tissue engineering applications. Therefore, material diversity and cross-linking strategies should be the focus of future research.

Secondly, most hydrogel composites are produced from simple mixing of different components at different weight ratios, which can induce severe agglomeration of reinforcements inside the hydrogel matrix. Poorly distributed reinforcements directly affect the performance of the hydrogel composite, thus new strategies for obtaining a uniform distribution or alignment of reinforcements are impertinent for practical applications involving hydrogel composites.

Finally, the alignment or continuity of the reinforcements are also restricted to the X-Y plane because of the layer-by-layer additive fabrication process of 3D printing systems. Printing paths are only allowed in two dimensions (X- and Y-axis), and the mechanical strengthening is also limited to directions parallel with the printing paths. This is the reason why only simple shapes such as rod, bar, and dog-bone have been fabricated and evaluated using one-directional mechanical characterizations. For tissue engineering applications, implanted materials undergo complex loading conditions *in vivo*, and the mechanical properties of hydrogel composites are strongly dependent on their internal microstructure. Therefore, new 3D printing systems focusing on 3D alignment or continuity of internal reinforcements should be developed to improve the mechanical performance of hydrogel composites.

While many problems remain to be unsolved, various fascinating and promising results of the 3D printing system have been reported continuously, and hydrogel composite materials with enhanced printability, mechanical properties, and biological performances have been also designed and proposed. We expect that the classification of 3D printing systems, categorization of hydrogel composite materials, and their applications that have been discussed in this review article will provide a fundamental understanding of hydrogel composite materials and 3D printing systems,

and serve as a platform to design innovative combinations of materials and 3D printing techniques for emerging applications, such as cancer modeling and organ-on-a-chip models.

Conflict of Interest and Funding

No conflict of interest was reported by all authors. This research was supported by AcRF Tier 1 grant 2017-T1-001-246 (RG51/17) from Ministry of Education of Singapore, and Basic Science Research Program (No. 2015R1D1A1A01057311 & 2017R1A6A3A03008914) through the National Research Foundation of Korea (NRF) funded by the Ministry of Science, ICT & Future Planning.

References

1. Wang X, Jiang M, Zhou Z W, *et al.*, 2017, 3D printing of polymer matrix composites: A review and prospective. *Compos B Eng*, 110: 442–458. <http://dx.doi.org/10.1016/j.compositesb.2016.11.034>
2. Chua C K and Leong K F, 3D printing and additive manufacturing : Principles and applications, 4th ed. Singapore: World Scientific Publishing; 2015.
3. Billiet T, Vandenhaute M, Schelfhout J, *et al.*, 2012, A review of trends and limitations in hydrogel-rapid prototyping for tissue engineering. *Biomaterials*, 33(26): 6020–6041. <http://dx.doi.org/10.1016/j.biomaterials.2012.04.050>
4. Ballyns J J, Gleghorn J P, Niebrzydowski V, *et al.*, 2008, Image-guided tissue engineering of anatomically shaped implants via MRI and micro-CT using injection molding. *Tissue Eng Part A*, 14(7): 1195–1202. <http://dx.doi.org/10.1089/ten.tea.2007.0186>
5. Chia H N and Wu B M, 2015, Recent advances in 3D printing of biomaterials. *J Biol Eng*, 9(1): 4 <http://dx.doi.org/10.1186/S13036-015-0001-4>
6. Seyednejad H, Gawlitta D, Kuiper R V, *et al.*, 2012, *In vivo* biocompatibility and biodegradation of 3D-printed porous scaffolds based on a hydroxyl-functionalized poly(epsilon-caprolactone). *Biomaterials*, 33(17): 4309–4318. <http://dx.doi.org/10.1016/j.biomaterials.2012.03.002>
7. Wu G H and Hsu S H, 2015, Review: Polymeric-Based 3D printing for tissue engineering. *J Med Bioeng*, 35(3): 285–292. <http://dx.doi.org/10.1007/s40846-015-0038-3>
8. Utech S and Boccaccini A R, 2016, A review of hydrogel-based composites for biomedical applications: Enhancement of hydrogel properties by addition of rigid inorganic fillers. *J Mater Sci*, 51(1): 271–310. <http://dx.doi.org/10.1007/s10853-015-9382-5>
9. Gaharwar A K, Peppas N A and Khademhosseini A, 2014, Nanocomposite hydrogels for biomedical applications. *Biotechnol Bioeng*, 111(3): 441–453. <http://dx.doi.org/10.1002/bit.25160>
10. Xu K, Wang J H, Chen Q, *et al.*, 2008, Spontaneous volume transition of polyampholyte nanocomposite hydrogels based on pure electrostatic interaction. *J Colloid Interface Sci*, 321(2): 272–278. <http://dx.doi.org/10.1016/j.jcis.2008.02.024>
11. Kabiri K, Omidian H, Zohuriaan-Mehr M J, *et al.*, 2011, Superabsorbent hydrogel composites and nanocomposites: A review. *Polym Compos*, 32(2): 277–289. <http://dx.doi.org/10.1002/pc.21046>
12. Thoniyot P, Tan M J, Karim A A, *et al.*, 2015, Nanoparticle-Hydrogel composites: Concept, design, and applications of these promising, multi-functional materials. *Adv Sci*, 2(1–2). <http://dx.doi.org/10.1002/AdvS.201400010>
13. Lee J W, Kim S Y, Kim S S, *et al.*, 1999, Synthesis and characteristics of interpenetrating polymer network hydrogel composed of chitosan and poly(acrylic acid). *J Appl Polym Sci*, 73(1): 113–120. [http://dx.doi.org/10.1002/\(SICI\)1097-4628\(19990705\)73:1<113::AID-APP13>3.0.CO;2-D](http://dx.doi.org/10.1002/(SICI)1097-4628(19990705)73:1<113::AID-APP13>3.0.CO;2-D)
14. Ehrburger P and Donnet J B, 1980, Interface in composite-materials. *Philos Trans A Math Phys Eng Sci*, 294(1411): 495–505. <http://dx.doi.org/10.1098/rsta.1980.0059>
15. Jeong S H, Koh Y H, Kim S W, *et al.*, 2016, Strong and biostable hyaluronic acid-calcium phosphate nanocomposite hydrogel *via in situ* precipitation process. *Biomacromolecules*, 17(3): 841–851. <http://dx.doi.org/10.1021/acs.biomac.5b01557>
16. Wust S, Godla M E, Muller R, *et al.*, 2014, Tunable hydrogel composite with two-step processing in combination with innovative hardware upgrade for cell-based three-dimensional bioprinting. *Acta Biomater*, 10(2): 630–640. <http://dx.doi.org/10.1016/j.actbio.2013.10.016>
17. Duan B, Hockaday L A, Kang K H, *et al.*, 2013, 3D Bioprinting of heterogeneous aortic valve conduits with alginate/gelatin hydrogels. *J Biomed Mater Res A*, 101(5): 1255–1264. <http://dx.doi.org/10.1002/jbm.a.34420>
18. Melchels F P W, Feijen J and Grijpma D W, 2010, A review on stereolithography and its applications in biomedical engineering. *Biomaterials*, 31(24): 6121–6130. <http://dx.doi.org/10.1016/j.biomaterials.2010.04.050>
19. Bertsch A, Jiguet S, Bernhard P, *et al.*, 2003, Microstereolithography: A review. *Rapid Prototyping Technologies*, 758: 3–15.
20. Beluze L, Bertsch A and Renaud P, 1999, Microstereolithography: A new process to build complex 3D objects. *Design*,

- Test, and Microfabrication of Mems and Moems, Pts 1 and 2*, 3680: 808–817. <http://dx.doi.org/10.1117/12.341277>
21. Choi J S, Kang H W, Lee I H, et al., 2009, Development of micro-stereolithography technology using a UV lamp and optical fiber. *Int J Adv Manuf Technol*, 41(3–4): 281–286. <http://dx.doi.org/10.1007/s00170-008-1461-1>
 22. Bertsch A, Renaud P, Vogt C, et al., 2000, Rapid prototyping of small size objects. *Rapid Prototyp J*, 6(4): 259–266. <http://dx.doi.org/10.1108/13552540010373362>
 23. Sun C, Fang N, Wu D M, et al., 2005, Projection micro-stereolithography using digital micro-mirror dynamic mask. *Sens Actuators A Phys*, 121(1): 113–120. <http://dx.doi.org/10.1016/j.sna.2004.12.011>
 24. Ambrosio L, Biomedical composites, 2nd ed. UK: Woodhead Publishing; 2010.
 25. Maruo Sand Ikuta K, 2002, Submicron stereolithography for the production of freely movable mechanisms by using single-photon polymerization. *Sens Actuators A Phys*, 100(1): 70–76. [http://dx.doi.org/10.1016/S0924-4247\(02\)00043-2](http://dx.doi.org/10.1016/S0924-4247(02)00043-2)
 26. Lee K S, Kim R H, Yang D Y, et al., 2008, Advances in 3D nano/microfabrication using two-photon initiated polymerization. *Prog Polym Sci*, 33(6): 631–681. <http://dx.doi.org/10.1016/j.progpolymsci.2008.01.001>
 27. Weiss T, Hildebrand G, Schade R, et al., 2009, Two-Photon polymerization for microfabrication of three-dimensional scaffolds for tissue engineering application. *Eng Life Sci*, 9(5): 384–390. <http://dx.doi.org/10.1002/else.200900002>
 28. Ostendorf A and Chichkov B N, 2006, Two-photon polymerization: A new approach to micromachining. *Photonics Spectra*, 40(10): 72–80.
 29. Hutmacher D W, Sittinger M and Risbud M V, 2004, Scaffold-based tissue engineering: Rationale for computer-aided design and solid free-form fabrication systems. *Trends Biotechnol*, 22(7): 354–362. <http://dx.doi.org/10.1016/j.tibtech.2004.05.006>
 30. Bikas H, Stavropoulos P and Chryssolouris G, 2016, Additive manufacturing methods and modelling approaches: A critical review. *Int J Adv Manuf Technol*, 83(1–4): 389–405. <http://dx.doi.org/10.1007/s00170-015-7576-2>
 31. Anitha R, Arunachalam S and Radhakrishnan P, 2001, Critical parameters influencing the quality of prototypes in fused deposition modelling. *J Mater Process Technol*, 118(1): 385–388. [http://dx.doi.org/10.1016/S0924-0136\(01\)00980-3](http://dx.doi.org/10.1016/S0924-0136(01)00980-3)
 32. Xiong Z, Yan Y, Zhang R, et al., 2001, Fabrication of porous poly (L-lactic acid) scaffolds for bone tissue engineering via precise extrusion. *Scr Mater*, 45(7): 773–779. [http://dx.doi.org/10.1016/S1359-6462\(01\)01094-6](http://dx.doi.org/10.1016/S1359-6462(01)01094-6)
 33. Greulich M, Greul M and Pintat T, 1995, Fast, functional prototypes via multiphase jet solidification. *Rapid Prototyp J*, 1(1): 20–25. <http://dx.doi.org/10.1108/13552549510146649>
 34. Shor L, Güçeri S, Chang R, et al., 2009, Precision extruding deposition (PED) fabrication of polycaprolactone (PCL) scaffolds for bone tissue engineering. *Biofabrication*, 1(1): 015003. <http://dx.doi.org/10.1088/1758-5082/1/1/015003>
 35. Torres J, Cotel J, Karl J, et al., 2015, Mechanical property optimization of FDM PLA in shear with multiple objectives. *JOM*, 67(5): 1183–1193. <http://dx.doi.org/10.1007/s11837-015-1367-y>
 36. Yeong W Y, Chua C K, Leong K F, et al., 2004, Rapid prototyping in tissue engineering: Challenges and potential. *Trends Biotechnol*, 22(12): 643–652. <http://dx.doi.org/10.1016/j.tibtech.2004.10.004>
 37. Gates R D, Baghdasarian G and Muscatine L, 1992, Temperature stress causes host-cell detachment in symbiotic cnidarians-implications for coral bleaching. *Biol Bull*, 182(3): 324–332. <http://dx.doi.org/10.2307/1542252>
 38. Landers R and Mülhaupt R, 2000, Desktop manufacturing of complex objects, prototypes and biomedical scaffolds by means of computer-assisted design combined with computer-guided 3D plotting of polymers and reactive oligomers. *Macromol Mater Eng*, 282(1): 17–21. [http://dx.doi.org/10.1002/1439-2054\(20001001\)282:1<17::AID-MAME17>3.0.CO;2-8](http://dx.doi.org/10.1002/1439-2054(20001001)282:1<17::AID-MAME17>3.0.CO;2-8)
 39. Billiet T, Gevaert E, De Schryver T, et al., 2014, The 3D printing of gelatin methacrylamide cell-laden tissue-engineered constructs with high cell viability. *Biomaterials*, 35(1): 49–62. <http://dx.doi.org/10.1016/j.biomaterials.2013.09.078>
 40. Luo Y, Lode A, Akkineni A R, et al., 2015, Concentrated gelatin/alginate composites for fabrication of predesigned scaffolds with a favorable cell response by 3D plotting. *RSC Adv*, 5(54): 43480–43488. <http://dx.doi.org/10.1039/C5RA04308E>
 41. Akkineni A R, Luo Y, Schumacher M, et al., 2015, 3D plotting of growth factor loaded calcium phosphate cement scaffolds. *Acta Biomater*, 27: 264–274. <http://dx.doi.org/10.1016/j.actbio.2015.08.036>
 42. Yilgor P, Sousa R A, Reis R L, et al., 3D plotted PCL scaffolds for stem cell based bone tissue engineering, *Macromol Symp*, 2008. *Wiley Online Library*, 269:92–99. <http://dx.doi.org/10.1002/masy.200850911>
 43. Landers R and Mülhaupt R, 2000, Desktop manufacturing

- of complex objects, prototypes and biomedical scaffolds by means of computer-assisted design combined with computer-guided 3D plotting of polymers and reactive oligomers. *Macromol Mater Eng*, 282(9): 17–21. [http://dx.doi.org/10.1002/1439-2054\(20001001\)282:1<17::Aid-Mame17>3.0.Co;2-8](http://dx.doi.org/10.1002/1439-2054(20001001)282:1<17::Aid-Mame17>3.0.Co;2-8)
44. Smay J E, Gratson G M, Shepherd R F, *et al.*, 2002, Directed colloidal assembly of 3D periodic structures. *Adv Mater*, 14(18): 1279–1283.
 45. Ahn B Y, Duoss E B, Motala M J, *et al.*, 2009, Omnidirectional printing of flexible, stretchable, and spanning silver microelectrodes. *Science*, 323(5921): 1590–1593. <https://dx.doi.org/10.1126/science.1168375>
 46. Vozzi G, Previti A, De Rossi D, *et al.*, 2002, Microsyringe-based deposition of two-dimensional and three-dimensional polymer scaffolds with a well-defined geometry for application to tissue engineering. *Tissue Eng*, 8(6): 1089–1098. <https://dx.doi.org/10.1089/107632702320934182>
 47. Tartarisco G, Gallone G, Carpi F, *et al.*, 2009, Polyurethane unimorph bender microfabricated with pressure assisted microsyringe (PAM) for biomedical applications. *Mater Sci Eng C Mater Biol Appl*, 29(6): 1835–1841. <https://dx.doi.org/10.1016/j.msec.2009.02.017>
 48. Xiong Z, Yan Y, Wang S, *et al.*, 2002, Fabrication of porous scaffolds for bone tissue engineering via low-temperature deposition. *Scr Mater*, 46(11): 771–776. [https://dx.doi.org/10.1016/S1359-6462\(02\)00071-4](https://dx.doi.org/10.1016/S1359-6462(02)00071-4)
 49. Liu L, Xiong Z, Zhang R, *et al.*, 2009, A novel osteochondral scaffold fabricated via multi-nozzle low-temperature deposition manufacturing. *J Bioact Compat Polym*, 24(1): 18–30. <https://dx.doi.org/10.1177/0883911509102347>
 50. Vadnere M, Amidon G, Lindenbaum S, *et al.*, 1984, Thermodynamic studies on the gel-sol transition of some pluronic polyols. *Int J Pharm*, 22(2–3): 207–218. [https://dx.doi.org/10.1016/0378-5173\(84\)90022-X](https://dx.doi.org/10.1016/0378-5173(84)90022-X)
 51. Kim J Y and Cho D-W, 2009, Blended PCL/PLGA scaffold fabrication using multi-head deposition system. *Microelectron Eng*, 86(4): 1447–1450. <https://dx.doi.org/10.1016/j.mee.2008.11.026>
 52. Domingos M, Dinucci D, Cometa S, *et al.*, 2009, Polycaprolactone scaffolds fabricated via bioextrusion for tissue engineering applications. *Int J Biomater*, 2009(1687–8787) : 239643. <https://dx.doi.org/10.1155/2009/239643>
 53. Lam C, Olkowski R, Swieszkowski W, *et al.*, 2008, Mechanical and *in vitro* evaluations of composite PLDLLA/TCP scaffolds for bone engineering. *Virtual Phys Prototyp*, 3(4): 193–197. <https://dx.doi.org/10.1080/17452750802551298>
 54. Lim T, Bang C, Chian K, *et al.*, 2008, Development of cryogenic prototyping for tissue engineering. *Virtual Phys Prototyp*, 3(1): 25–31. <https://dx.doi.org/10.1080/17452750701799303>
 55. Bang Pham C, Fai Leong K, Chiun Lim T, *et al.*, 2008, Rapid freeze prototyping technique in bio-plotters for tissue scaffold fabrication. *Rapid Prototyp J*, 14(4): 246–253. <https://dx.doi.org/10.1108/13552540810896193>
 56. Lu L, Zhang Q, Wootton D, *et al.*, 2010, A novel sucrose porogen-based solid freeform fabrication system for bone scaffold manufacturing. *Rapid Prototyp J*, 16(5): 365–376. <https://dx.doi.org/10.1108/13552541011065768>
 57. Cima M, Sachs E, Fan T, *et al.*, Three-dimensional printing techniques. US patent 5387380, 1995 July 2.
 58. Mei J, Lovell M, Rand Mickle M H, 2005, Formulation and processing of novel conductive solution inks in continuous inkjet printing of 3-D electric circuits. *IEEE Trans Compon Packaging Manuf Technol*, 28(3): 265–273. <https://dx.doi.org/10.1109/TEPM.2005.852542>
 59. Saunders R E, Gough J E and Derby B, 2008, Delivery of human fibroblast cells by piezoelectric drop-on-demand inkjet printing. *Biomaterials*, 29(2): 193–203. <https://dx.doi.org/10.1016/j.biomaterials.2007.09.032>
 60. Nakamura M, Kobayashi A, Takagi F, *et al.*, 2005, Biocompatible inkjet printing technique for designed seeding of individual living cells. *Tissue Eng*, 11(11–12): 1658–1666. <https://dx.doi.org/10.1089/ten.2005.11.1658>
 61. Cui X, Dean D, Ruggeri Z M, *et al.*, 2010, Cell damage evaluation of thermal inkjet printed Chinese hamster ovary cells. *Biotechnol Bioeng*, 106(6): 963–969. <https://dx.doi.org/10.1002/bit.22762>
 62. Leukers B, Gülkan H, Irsen S H, *et al.*, 2005, Hydroxyapatite scaffolds for bone tissue engineering made by 3D printing. *J MATER SCI-MATER M*, 16(12): 1121–1124. <https://dx.doi.org/10.1007/s10856-005-4716-5>
 63. Inzana J A, Olvera D, Fuller S M, *et al.*, 2014, 3D printing of composite calcium phosphate and collagen scaffolds for bone regeneration. *Biomaterials*, 35(13): 4026–4034. <https://dx.doi.org/10.1016/j.biomaterials.2014.01.064>
 64. Levy A, Miriyev A, Elliott A, *et al.*, 2017, Additive manufacturing of complex-shaped graded TiC/steel composites. *Mater Design*, 118: 198–203. <https://dx.doi.org/10.1016/j.matdes.2017.01.024>
 65. Pfister A, Landers R, Laib A, *et al.*, 2004, Biofunctional rapid prototyping for tissue-engineering applications: 3D bioplotting versus 3D printing. *J Polym Sci Pol Chem*, 42(3): 624–638. <https://dx.doi.org/10.1002/pola.10807>

66. Boland T, Tao X, Damon B J, et al., 2007, Drop-on-demand printing of cells and materials for designer tissue constructs. *Mater Sci Eng C Mater Biol Appl*, 27(3): 372–376. <https://dx.doi.org/10.1016/j.msec.2006.05.047>
67. Sun J, Ng J H, Fuh Y H, et al., 2009, Comparison of micro-dispensing performance between micro-valve and piezoelectric printhead. *Microsyst Technol*, 15(9): 1437–1448. <https://dx.doi.org/10.1007/s00542-009-0905-3>
68. Zusiak S P and Leach J B, 2010, Hydrolytically degradable poly (ethylene glycol) hydrogel scaffolds with tunable degradation and mechanical properties. *Biomacromolecules*, 11(5): 1348–1357. <https://dx.doi.org/10.1021/bm100137q>
69. Killion J A, Geever L M, Devine D M, et al., 2014, Compressive strength and bioactivity properties of photopolymerizable hybrid composite hydrogels for bone tissue engineering. *Int J Polym Mater Po*, 63(13): 641–650. <https://dx.doi.org/10.1080/00914037.2013.854238>
70. Bakarich S E, Gorkin R, Gately R, et al., 2017, 3D printing of tough hydrogel composites with spatially varying materials properties. *Addit Manuf*, 14: 24–30. <https://dx.doi.org/10.1016/j.addma.2016.12.003>
71. Zhao L, Lee V K, Yoo S-S, et al., 2012, The integration of 3-D cell printing and mesoscopic fluorescence molecular tomography of vascular constructs within thick hydrogel scaffolds. *Biomaterials*, 33(21): 5325–5332. <http://dx.doi.org/10.1016/j.biomaterials.2012.04.004>
72. Hong S, Sycks D, Chan H F, et al., 2015, 3D printing of highly stretchable and tough hydrogels into complex, cellularized structures. *Adv Mater*, 27(27): 4035–4040. <http://dx.doi.org/10.1002/adma.201501099>
73. Markstedt K, Mantas A, Tournier I, et al., 2015, 3D bioprinting human chondrocytes with nanocellulose–alginate bioink for cartilage tissue engineering applications. *Biomacromolecules*, 16(5): 1489–1496. <http://dx.doi.org/10.1021/acs.biomac.5b00188>
74. Rutz A L, Hyland K E, Jakus A E, et al., 2015, A multimaterial bioink method for 3D printing tunable, cell-compatible hydrogels. *Adv Mater*, 27(9): 1607–1614. <http://dx.doi.org/10.1002/adma.201405076>
75. Xu M, Wang X, Yan Y, et al., 2010, An cell-assembly derived physiological 3D model of the metabolic syndrome, based on adipose-derived stromal cells and a gelatin/alginate/fibrinogen matrix. *Biomaterials*, 31(14): 3868–3877. <http://dx.doi.org/10.1016/j.biomaterials.2010.01.111>
76. Akkineni A R, Ahlfeld T, Funk A, et al., 2016, Highly concentrated alginate-gellan gum composites for 3D plotting of complex tissue engineering scaffolds. *Polymers*, 8(5): 170. <http://dx.doi.org/10.3390/polym8050170>
77. Boere K W, Blokzijl M M, Visser J, et al., 2015, Biofabrication of reinforced 3D-scaffolds using two-component hydrogels. *J Mater Chem B Mater Biol Med*, 3(46): 9067–9078. <http://dx.doi.org/10.1039/C5TB01645B>
78. Censi R, Schuurman W, Malda J, et al., 2011, A printable photopolymerizable thermosensitive p (HPMAm-lactate)-PEG hydrogel for tissue engineering. *Adv Funct Mater*, 21(10): 1833–1842. <http://dx.doi.org/10.1002/adfm.201002428>
79. Osterbur L, 2013, 3D printing of hyaluronic acid scaffolds for tissue engineering applications [Internet]. Available from: <http://hdl.handle.net/2142/44207>
80. Wang X, Cui T, Yan Y, et al., 2009, Peroneal nerve regeneration using a unique bilayer polyurethane-collagen guide conduit. *J Bioact Compat Polym*, 24(2): 109–127. <http://dx.doi.org/10.1177/0883911508101183>
81. Mogas-Soldevila L, Duro-Royo J and Oxman N, 2014, Water-based robotic fabrication: Large-Scale additive manufacturing of functionally graded hydrogel composites via multichamber extrusion. *3D Print Addit Manuf*, 1(3): 141–151. <http://dx.doi.org/10.1089/3dp.2014.0014>
82. Shie M-Y, Chang W-C, Wei L-J, et al., 2017, 3D printing of cytocompatible water-based light-cured polyurethane with hyaluronic acid for cartilage tissue engineering applications. *Materials*, 10(2): 136. <http://dx.doi.org/10.3390/ma10020136>
83. Wang X H, Tolba E, Schroder H C, et al., 2014, Effect of bioglass on growth and biomineralization of Saos-2 cells in hydrogel after 3D cell bioprinting. *Plos One*, 9(11): e112497 <http://dx.doi.org/10.1371/journal.pone.0112497>
84. Sayyar S, Gambhir S, Chung J, et al., 2017, 3D printable conducting hydrogels containing chemically converted graphene. *Nanoscale*, 9(5): 2038–2050. <http://dx.doi.org/10.1039/c6nr07516a>
85. Demirtas T T, Irmak G and Gumusderelioglu M, 2017, A bioprintable form of chitosan hydrogel for bone tissue engineering. *Biofabrication*, 9(3): 035003. <http://dx.doi.org/10.1088/1758-5090/Aa7b1d>
86. Skardal A, Zhang J X, McCoard L, et al., 2010, Dynamically crosslinked gold nanoparticle–Hyaluronan hydrogels. *Adv Mater*, 22(42): 4736. <http://dx.doi.org/10.1002/adma.201001436>
87. Fedorovich N E, Wijnberg H M, Dhert W J, et al., 2011, Distinct tissue formation by heterogeneous printing of osteo- and endothelial progenitor cells. *Tissue Eng Part A*, 17(15–16):

- 2113–2121. <http://dx.doi.org/10.1089/ten.tea.2011.0019>
88. Panhuis M I H, Heurtematte A, Small W R, *et al.*, 2007, Inkjet printed water sensitive transparent films from natural gum-carbon nanotube composites. *Soft Matter*, 3(7): 840–843. <http://dx.doi.org/10.1039/b704368f>
 89. Heo D N, Castro N J, Lee S J, *et al.*, 2017, Enhanced bone tissue regeneration using a 3D printed microstructure incorporated with a hybrid nano hydrogel. *Nanoscale*, 9(16): 5055–5062. <http://dx.doi.org/10.1039/c6nr09652b>
 90. Zhu W, Holmes B, Glazer R I, *et al.*, 2016, 3D printed nanocomposite matrix for the study of breast cancer bone metastasis. *Nanomedicine*, 12(1): 69–79. <http://dx.doi.org/10.1016/j.nano.2015.09.010>
 91. Castro N J, O'Brien J and Zhang L G, 2015, Integrating biologically inspired nanomaterials and table-top stereolithography for 3D printed biomimetic osteochondral scaffolds. *Nanoscale*, 7(33): 14010–14022. <http://dx.doi.org/10.1039/c5nr03425f>
 92. Gladman A S, Matsumoto E A, Nuzzo R G, *et al.*, 2016, Biomimetic 4D printing. *Nat Mater*, 15(4): 413–418. <http://dx.doi.org/10.1038/NMAT4544>
 93. Narayanan L K, Huebner P, Fisher M B, *et al.*, 2016, 3D-Bioprinting of polylactic acid (PLA) nanofiber-alginate hydrogel bioink containing human adipose-derived stem cells. *ACS Biomater Sci Eng*, 2(10): 1732–1742. <http://dx.doi.org/10.1021/acsbomaterials.6b00196>
 94. Agrawal A, Rahbar N and Calvert P D, 2013, Strong fiber-reinforced hydrogel. *Acta Biomaterialia*, 9(2): 5313–5318. <http://dx.doi.org/10.1016/j.actbio.2012.10.011>
 95. Bakarich S E, Gorkin R, Panhuis M I H, *et al.*, 2014, Three-dimensional printing fiber reinforced hydrogel composites. *ACS Appl Mater Interfaces*, 6(18): 15998–16006. <http://dx.doi.org/10.1021/am503878d>
 96. Jin Y, Liu C, Chai W, *et al.*, 2017, Self-Supporting nanoclay as internal scaffold material for direct printing of soft hydrogel composite structures in air. *ACS Appl Mater Interfaces*, 9(20):17456–17465. <http://dx.doi.org/10.1021/acsami.7b03613>
 97. Zhai X, Ma Y, Hou C, *et al.*, 2017, 3D-printed high strength bioactive supramolecular polymer/clay nanocomposite hydrogel scaffold for bone regeneration. *ACS Biomater Sci Eng*, 3(6): 1109–1118. <http://dx.doi.org/10.1021/acsbomaterials.7b00224>
 98. Ahlfeld T, Cidonio G, Kilian D, *et al.*, 2017, Development of a clay based bioink for 3D cell printing for skeletal application. *Biofabrication*, 9(3). <http://dx.doi.org/10.1088/1758-5090/aa7e96>
 99. Egorov A A, Fedotov A Y, Mironov A V, *et al.*, 2016, 3D printing of mineral-polymer bone substitutes based on sodium alginate and calcium phosphate. *Beilstein J Nanotechnol*, 7(1): 1794–1799. <http://dx.doi.org/10.3762/bjnano.7.172>
 100. Rawat K, Agarwal S, Tyagi A, *et al.*, 2014, Aspect ratio dependent cytotoxicity and antimicrobial properties of nanoclay. *Appl Biochem Biotechnol*, 174(3): 936–944. <http://dx.doi.org/10.1007/s12010-014-0983-2>
 101. Mourchid A, Delville A, Lambard J, *et al.*, 1995, Phase diagram of colloidal dispersions of anisotropic charged particles: Equilibrium properties, structure, and rheology of laponite suspensions. *Langmuir*, 11(6): 1942–1950. <http://dx.doi.org/10.1021/la00006a020>
 102. Su D, Jiang L, Chen X, *et al.*, 2016, Enhancing the gelation and bioactivity of injectable silk fibroin hydrogel with laponite nanoplatelets. *ACS Appl Mater Interfaces*, 8(15): 9619–9628. <http://dx.doi.org/10.1021/acsami.6b00891>
 103. Liu Y, Meng H, Konst S, *et al.*, 2014, Injectable dopamine-modified poly (ethylene glycol) nanocomposite hydrogel with enhanced adhesive property and bioactivity. *ACS Appl Mater Interfaces*, 6(19): 16982–16992. <http://dx.doi.org/10.1021/am504566v>
 104. Demirtaş T T, Irmak G and Gümüşderelioğlu M, 2017, A bioprintable form of chitosan hydrogel for bone tissue engineering. *Biofabrication*, 9(3): 035003. <http://dx.doi.org/10.1088/1758-5090/aa7b1d>
 105. Diogo G, Gaspar V, Serra I, *et al.*, 2014, Manufacture of β -TCP/alginate scaffolds through a Fab@ home model for application in bone tissue engineering. *Biofabrication*, 6(2): 025001. <http://dx.doi.org/10.1088/1758-5082/6/2/025001>
 106. Kang M-H, Jang T-S, Jung H-D, *et al.*, 2016, Poly (ether imide)-silica hybrid coatings for tunable corrosion behavior and improved biocompatibility of magnesium implants. *Bioact Mater*, 11(3): 035003. <http://dx.doi.org/10.1088/1748-6041/11/3/035003>
 107. Lee H, Kim Y, Kim S, *et al.*, 2014, Mineralized biomimetic collagen/alginate/silica composite scaffolds fabricated by a low-temperature bio-plotting process for hard tissue regeneration: fabrication, characterisation and *in vitro* cellular activities. *J Mater Chem B Mater Biol Med*, 2(35): 5785–5798. <http://dx.doi.org/10.1039/C4TB00931B>
 108. Wang X, Tolba E, Schröder H C, *et al.*, 2014, Effect of bioglass on growth and biomineralization of SaOS-2 cells in hydrogel after 3D cell bioprinting. *PLoS One*, 9(11): e112497. <http://dx.doi.org/10.1371/journal.pone.0112497>
 109. Huey D J, Hu J C and Athanasiou K A, 2012, Unlike bone,

- cartilage regeneration remains elusive. *Science*, 338(6109): 917–921. <http://dx.doi.org/10.1126/science.1222454>
110. Bartnikowski M, Akkineni A R, Gelinsky M, et al., 2016, A hydrogel model incorporating 3D-plotted hydroxyapatite for osteochondral tissue engineering. *Materials*, 9(4): 285. <http://dx.doi.org/10.3390/ma9040285>
 111. Kundu J, Shim J H, Jang J, et al., 2015, An additive manufacturing-based PCL–alginate–chondrocyte bioprinted scaffold for cartilage tissue engineering. *J Tissue Eng Regen Med*, 9(11): 1286–1297. <http://dx.doi.org/10.1002/term.1682>
 112. Xu T, Binder K W, Albanna M Z, et al., 2012, Hybrid printing of mechanically and biologically improved constructs for cartilage tissue engineering applications. *Biofabrication*, 5(1): 015001. <http://dx.doi.org/10.1088/1758-5082/5/1/015001>
 113. Wei J, Wang J, Su S, et al., 2015, 3D printing of an extremely tough hydrogel. *RSC Adv*, 5(99): 81324–81329. <http://dx.doi.org/10.1039/C5RA16362E>
 114. Sugihara H, Toda S, Miyabara S, et al., 1991, Reconstruction of the skin in three-dimensional collagen gel matrix culture. *In Vitro Cell Dev Biol Anim*, 27(2): 142–146. <http://dx.doi.org/10.1007/BF02631000>
 115. Dorsett-Martin W A, 2004, Rat models of skin wound healing: A review. *Wound Repair Regen*, 12(6): 591–599. <http://dx.doi.org/10.1111/j.1067-1927.2004.12601.x>
 116. Skardal A, Mack D, Kapetanovic E, et al., 2012, Bioprinted amniotic fluid-derived stem cells accelerate healing of large skin wounds. *Stem Cells Transl Med*, 1(11): 792–802. <http://dx.doi.org/10.5966/sctm.2012-0088>
 117. Sayyar S, Murray E, Thompson B, et al., 2015, Processable conducting graphene/chitosan hydrogels for tissue engineering. *J Mater Chem B Mater Biol Med*, 3(3): 481–490. <http://dx.doi.org/10.1039/C4TB01636J>
 118. Suh J-K and Matthew H W, 2000, Application of chitosan-based polysaccharide biomaterials in cartilage tissue engineering: A review. *Biomaterials*, 21(24): 2589–2598. [http://dx.doi.org/10.1016/S0142-9612\(00\)00126-5](http://dx.doi.org/10.1016/S0142-9612(00)00126-5)
 119. Knowlton S, Yenilmez B, Anand S, et al., 2017, Photocrosslinking-based bioprinting: Examining crosslinking schemes. *Bioprinting*, 5: 10–18. <https://dx.doi.org/10.1016/j.bprint.2017.03.001>
 120. Nair K, Gandhi M, Khalil S, et al., 2009, Characterization of cell viability during bioprinting processes. *Biotechnol J*, 4(8): 1168–1177. <http://dx.doi.org/10.1002/biot.200900004>
 121. Arslan-Yildiz A, El Assal R, Chen P, et al., 2016, Towards artificial tissue models: Past, present, and future of 3D bioprinting. *Biofabrication*, 8(1): 014103. <http://dx.doi.org/10.1088/1758-5090/8/1/014103>
 122. Pereira R and Bartolo P J, 2015, 3D bioprinting of photocrosslinkable hydrogel constructs. *J Appl Polym Sci*, 132(48): 42458. <http://dx.doi.org/10.1002/App.42458>
 123. Kirchmayer D M, Gorkin R and Panhuis M I H, 2015, An overview of the suitability of hydrogel-forming polymers for extrusion-based 3D-printing. *J Mater Chem B Mater Biol Med*, 3(20): 4105–4117. <http://dx.doi.org/10.1039/c5tb00393h>
 124. Chirag Khatiwala R L, Benjamin Shepherd, Scott Dorfman, et al., 2012, 3D cell bioprinting for regenerative medicine research and therapies. *Gene Ther Regul*, 7(1): 1230004. <http://dx.doi.org/10.1142/S1568558611000301>
 125. Wang Z J, Jin X, Dai R, et al., 2016, An ultrafast hydrogel photocrosslinking method for direct laser bioprinting. *RSC Adv*, 6(25): 21099–21104. <http://dx.doi.org/10.1039/c5ra24910d>
 126. Armstrong J P K, Burke M, Carter B M, et al., 2016, 3D bioprinting using a templated porous bioink. *Adv Healthc Mater*, 5(14): 1724–1730. <http://dx.doi.org/10.1002/adhm.201600022>
 127. Cui X F, Breitenkamp K, Finn M G, et al., 2012, Direct human cartilage repair using three-dimensional bioprinting technology. *Tissue Eng Part A*, 18(11–12): 1304–1312. <http://dx.doi.org/10.1089/ten.tea.2011.0543>
 128. Fedorovich N E, Oudshoorn M H, van Geemen D, et al., 2009, The effect of photopolymerization on stem cells embedded in hydrogels. *Biomaterials*, 30(3): 344–353. <http://dx.doi.org/10.1016/j.biomaterials.2008.09.037>
 129. Folkman J and Hochberg M, 1973, Self-regulation of growth in three dimensions. *J Exp Med*, 138(4): 745–753.
 130. Li S, Xiong Z, Wang X, et al., 2009, Direct fabrication of a hybrid cell/hydrogel construct by a double-nozzle assembling technology. *J Bioact Compat Polym*, 24(3): 249–265. <http://dx.doi.org/10.1016/j.biomaterials.2016.07.038>
 131. Jia W, Gungor-Ozkerim P S, Zhang Y S, et al., 2016, Direct 3D bioprinting of perfusable vascular constructs using a blend bioink. *Biomaterials*, 106: 58–68. <http://dx.doi.org/10.1016/j.biomaterials.2016.07.038>
 132. Skardal A, Zhang J and Prestwich G D, 2010, Bioprinting vessel-like constructs using hyaluronan hydrogels crosslinked with tetrahedral polyethylene glycol tetracrylates. *Biomaterials*, 31(24): 6173–6181. <http://dx.doi.org/10.1016/j.biomaterials.2010.04.045>
 133. Dolati F, Yu Y, Zhang Y, et al., 2014, *In vitro* evaluation of carbon-nanotube-reinforced bioprintable vascular conduits. *Nanotechnology*, 25(14): 145101. <http://dx.doi.org/10.1088/0957-4484/25/14/145101>

134. Gao B, Yang Q Z, Zhao X, *et al.*, 2016, 4D bioprinting for biomedical applications. *Trends Biotechnol*, 34(9): 746–756. <http://dx.doi.org/10.10164.tibtech.2016.03.004>
135. Weiss R A, Izzo E and Mandelbaum S, 2008, New design of shape memory polymers: Mixtures of an elastomeric ionomer and low molar mass fatty acids and their salts. *Macromolecules*, 41(9): 2978–2980. <http://dx.doi.org/10.1021/ma8001774>
136. Leist S K and Zhou J, 2016, Current status of 4D printing technology and the potential of light-reactive smart materials as 4D printable materials. *Virtual Phys Prototyp*, 11(4): 249–262. <http://dx.doi.org/10.1080/17452759.2016.1198630>
137. He H Y, Guan J J and Lee J L, 2006, An oral delivery device based on self-folding hydrogels. *J Control Release*, 110(2): 339–346. <http://dx.doi.org/10.1016/j.jconrel.2005.10.017>
138. Khoo Z X, Teoh J E M, Liu Y, *et al.*, 2015, 3D printing of smart materials: A review on recent progresses in 4D printing. *Virtual Phys Prototyp*, 10(3): 103–122. <http://dx.doi.org/10.1080/17452759.2015.1097054>
139. He Y, Wu Y, Fu J Z, *et al.*, 2016, Developments of 3D printing microfluidics and applications in chemistry and biology: A review. *Electroanalysis*, 28(8): 1658–1678. <http://dx.doi.org/10.1002/elan.201600043>
140. Lee V K, Lanzi A M, Ngo H, *et al.*, 2014, Generation of multi-scale vascular network system within 3D hydrogel using 3D bio-printing technology. *Cell Mol Bioeng*, 7(3): 460–472. <http://dx.doi.org/10.1007/s12195-014-0340-0>